Secondary Flows in Rivers

1

Secondary Flows in Rivers: Theoretical Framework, Recent Advances, and Current Challenges

Vladimir Nikora and André G. Roy

1.1 INTRODUCTION

Water currents in rivers have fascinated and inspired researchers (and artists) for centuries, as reflected in numerous observations and paintings from ancient times (e.g., Rouse and Ince, 1963; Levi, 1995). Leonardo da Vinci's famous drawings are probably the most impressive and insightful examples of such observations. In his sketches and notes he highlighted a number of features of river flows whose signatures could be clearly observed at the water surface, especially behind obstacles and at stream confluences (Figure 1.1). 'Spiral' currents are particularly profound among these features and represent a key facet of nearly all of his water drawings. Using an analogy with curling hair, Leonardo summarized his observations as "Observe the motion of the surface of the water, how it resembles that of hair, which has two motions – one depends on the weight of the hair, the other on the direction of the curls; thus the water forms whirling eddies, one part following the impetus of the chief current, and the other following the incidental motion and return flow" (his written comment in Figure 1.1). It is fascinating how this description, given 500 years ago, is similar to a modern view of the mean flow structure as a superposition of the primary flow and the orthogonal secondary flows. Alternatively, Leonardo's comment may also be interpreted as the Reynolds decomposition of the instantaneous velocity into mean (i.e., time-averaged) and fluctuating turbulent components (Tsinober, 2009), although the first interpretation seems better justified.

Leonardo's astute comment on secondary flows was made well ahead of his time and it is nearly 400 years later that this phenomenon has been re-discovered by engineers and scientists working in hydraulics and theoretical fluid mechanics (e.g., Thomson, 1876; Francis, 1878; Wood, 1879;Cunningham, 1883; Stearns, 1883; Leliavski, 1894; Gibson, 1909; Joukowski, 1915). Their studies set up a background for the first fluid mechanical classification of the secondary flows proposed by Prandtl (1926). He suggested that "The phenomenon may be regarded as a combination of the main flow with a 'secondary flow' at right angles to it ..." and that this phenomenon combines two wide classes. The first class, known as Prandtl's secondary currents of the first kind, combines flow motions with streamwise mean (i.e., time-averaged) vorticity enhanced through vortex stretching. Secondary currents observed in curved pipe and river bends or meanders are typical examples provided by Prandtl to illustrate this type of secondary flow. Prandtl goes even further and proposes that the effect of secondary flows on sediment dynamics explains why "where they can, rivers always follow a winding course ('meandering')" (Prandtl, 1952, p. 147). The second class, often defined as Prandtl's secondary currents of the second kind, relates to secondary flows formed as a result of turbulence heterogeneity. These flows are often defined as turbulence-driven secondary currents and no channel curvature is required to generate them. Using rivers again as an example, Prandtl notes that "we may also mention the fact that small objects floating in rivers tend to move to the middle, which is explained by the existence of a surface current from the banks to the middle" (Prandtl, 1952, p. 148).

Typically, turbulence-generated longitudinal vorticity is much weaker than that in curved channels. However, even this seemingly mild three-dimensionality may introduce significant changes in the turbulence structure and should not be neglected. For instance, it is a common

Gravel-bed Rivers: Processes, Tools, Environments, First Edition. Edited by Michael Church, Pascale M. Biron and André G. Roy.

Figure 1.1 Leonardo da Vinci's Old Man with Water Studies (*c*. 1508–1509). Windsor, Royal Library, #12579.

claim in the experimental literature that the effects of the secondary flow on turbulence structure at the channel centreline are negligible, even in narrow channels. As a result, an assumption of a 2-D flow is often accepted based on the symmetry argument. This assumption ignores the cross-flow gradients of transverse velocities and turbulence parameters that may be (and often are) non-zero even at the channel centerline. Prandtl's secondary currents of the second kind typically occur at channel corners or at transverse bed roughness transitions. Recently, it has also been shown that this kind of secondary current may be formed in buoyancy-driven flows even in straight circular pipes (Hallez and Magnaudet, 2009), where normally this feature does not exist.

While turbulence acts to dissipate the secondary currents of the first kind, it represents a generating mechanism for the second kind of secondary currents. As a consequence, Prandtl's secondary currents of the second king are impossible in laminar flows, while Prandtl's first kind of secondary currents can be observed in both laminar and turbulent flows. Introduced rather intuitively, Prandtl's mechanism-based classification has survived extensive theoretical developments and is currently widely accepted as a starting point in considerations of secondary flows.

Prandtl's classification may additionally be supplemented with a topological classification that distinguishes two types of secondary flows: (1) non-helical cross-flows, and (2) helical flows (Bradshaw, 1987). Combining Prandtl's and Bradshaw's classifications, it is possible to distinguish at least four types of secondary currents: (i) Prandtl's first kind of cross-flow (non-helical); (ii) Prandtl's second kind of cross-flow (non-helical); (iii) Prandtl's first kind of helical flow; and (iv) Prandtl's second kind of helical flow. It is likely that in real river configurations all four types of secondary flow may be observed, either superimposed or separated in space and/or in time (e.g., topology and mechanisms of secondary currents at low flow may differ from those at flood stage; see Rhoads and Kenworthy, 1998). In some cases, one of these types may dominate the flow topology (e.g., Prandtl's first kind of helical flow may be dominant in some meandering rivers), while in other cases all four types can be equally significant (e.g., in braided rivers).

Although the great significance of secondary flows for river processes has long been recognised, their origin, mechanics, effects, and inter-relations with the primary mean flow and turbulence are still a matter of debate and continue to attract close attention from hydrologists, geomorphologists, engineers, and, recently, stream ecologists. It is not surprising therefore that the literature related to secondary flows in open channels is extensive (Scopus shows over 600 journal papers since 1990) and includes frequently appearing reviews reflecting the progress and highlighting unsolved issues.

Prandtl's secondary currents of the first kind, particularly related to meandering rivers, have been extensively discussed in Ikeda and Parker (1989), Rhoads and

Welford (1991), Blanckaert and de Vriend (2004), Seminara (2006, 2010), Camporeale *et al*. (2007), Abad and Garcia (2009a, 2009b), Ikeda and McEwan (2009), and Gyr (2010), among others. In terms of mechanical engineering applications, a comprehensive review of this class of secondary flows has been given by Bradshaw 1987, covering 3-D boundary layers, vortex flows, and jets in cross-flows. Prandtl's secondary currents of the second kind have also attracted significant attention and their discussion has been even more controversial than that of secondary currents of the first kind. Bradshaw's (1987) popular review only slightly touched on this topic (mainly for 3-D free jets and wall jets), probably because a comprehensive treatment of duct flows had already been given in the review by Demuren and Rodi (1984). In relation to open-channel flows, Nezu and Nakagawa's (1993) review of the turbulence-driven secondary currents is still the most comprehensive source, and a recent update of this excellent review is available (Nezu, 2005). There are also a number of in-depth papers reviewing complex flow patterns at river confluences where both kinds of Prandtl's secondary flows are present and are interlinked in a multifaceted way (e.g., Rhoads and Kenworthy, 1998; Bradbrook *et al*., 2000, 2001; Lane *et al*., 2000; Rhoads and Sukhodolov, 2001; Sukhodolov and Rhoads, 2001; Szupiany *et al*., 2009). The wide-ranging set of papers on this topic is also recorded in Rice *et al*. (2008), where extensive references and a thorough assessment of current and future research directions can be found.

The rapid development of measurement and numerical capabilities in recent years has brought new significant results and the authors feel that it may be useful to highlight recent progress in understanding secondary flows, as well as to identify research challenges and opportunities in studying this phenomenon, while keeping overlap with the previous reviews to the minimum. In particular, the focus of this chapter is on: (i) theoretical frameworks for studying secondary flows, (ii) interrelations between turbulence and secondary flows, and (iii) secondary flow effects on hydraulic resistance, sediment dynamics, and mixing. Examples from gravel-bed rivers will be presented. In addition to open-channel flows, some results related to conduits/ducts will also be considered as they are directly relevant to flows in ice-covered rivers (Ettema and Zabilansky, 2004; Buffin-Bélanger *et al*., 2009).

1.2 THEORETICAL FRAMEWORK

Most theoretical and conceptual approaches in studying secondary flows in ducts and open channels have been based on: (i) the time-(ensemble)-averaged momentum equation, (ii) the energy balance equation for the mean flow, (iii) the energy balance equation for turbulence, and (iv) the mean (i.e., time-averaged) vorticity equation. These equations stem from the Navier–Stokes (momentum) equation for instantaneous velocities and pressure, representing its different forms and, thus, essentially containing the same information. However, in various equations this information is presented differently, highlighting particular facets of secondary flows. Most theoretical and experimental studies have been based on one or another equation, rarely involving joint consideration of two or more equations, thus reflecting authors' preferences, specific research questions, and/or data availability. Such a narrowly focused approach could be a reason for discrepancies in the identification and interpretation of the physical mechanisms creating and maintaining secondary flows in straight and curved channels (an example is given in Section 1.2.2). It is therefore instructive to provide a comparative overview of these equations, as well as to highlight other forms of the Navier–Stokes equations which could provide additional insight into the mechanics of secondary flows. In this review, we use Cartesian coordinates, although curvilinear coordinates (cylindrical or natural) have also been extensively used, especially in dealing with curved channels. For our purpose, however, Cartesian coordinates should be sufficient. Equations in the following sections are written using the Cartesian index notation, where $i = 1$ is for x and velocity component u (along the flow), $i = 2$ is for y and velocity component v (across the flow), and $i = 3$ is for z and velocity component w (orthogonal to the bed into the fluid). The repeated indices (known as dummy indices) mean summation.

1.2.1 Reynolds-Averaged Navier–Stokes (RANS) Equation

The time-(ensemble) averaged momentum equation, widely known as the Reynolds-Averaged Navier–Stokes (RANS) equation or just the Reynolds equation, is a logical starting point in the analysis of secondary flows and also a suitable platform to define them. For the benefit of readers who are not closely familiar with this topic, this equation is given below:

$$\underbrace{\frac{\partial \bar{u}_i}{\partial t} + \bar{u}_j \frac{\partial \bar{u}_i}{\partial x_j}}_{\substack{\text{local} \\ \text{convective} \\ \text{accelerations}}} = \underbrace{g_i}_{\substack{\text{gravity} \\ \text{force}}} - \underbrace{\frac{1}{\rho}\frac{\partial \bar{p}}{\partial x_i}}_{\substack{\text{pressure} \\ \text{force}}} - \underbrace{\frac{\partial \overline{u_i' u_j'}}{\partial x_j}}_{\substack{\text{“turbulent”} \\ \text{force}}} + \underbrace{\frac{\partial}{\partial x_j}\left(\nu \frac{\partial \bar{u}_i}{\partial x_j}\right)}_{\substack{\text{viscous} \\ \text{shear} \\ \text{force}}} \quad (1.1)$$

where p is pressure, ρ is water density, ν is viscosity, overbar denotes time-(ensemble)- averaging and prime

denotes deviations of an instantaneous value of f from its mean value in the Reynolds decomposition, i.e., $f = \bar{f} + f'$.

For straight, steady uniform *2-D* open-channel flow, the conditions $\bar{u}_2 = \bar{u}_3 = \overline{u_1' u_2'} = \overline{u_2' u_3'} = 0$ apply and all derivatives in Equation (1.1) along and across the flow are equal to zero. In this case, the flow is defined by the longitudinal velocity $\bar{u}_1$ and vertical momentum flux towards the bed $\tau/\rho = -\overline{u_1' u_3'} + \nu \partial \bar{u}_1/\partial x_3 \approx -\overline{u_1' u_3'}$, while the vertical distribution of pressure may often be assumed to be hydrostatic (i.e., $g(H-z) >> [\overline{u_3' u_3'}(z_{ws}) - \overline{u_3' u_3'}(z)]$, where z_{ws} is the water surface elevation, H is water depth, and S is bed slope). The velocity component $\bar{u}_1$ defines the overall mass flux through the channel cross-section and therefore is often called the primary flow velocity, with $\tau/\rho = -\overline{u_1' u_3'}$ known as the primary Reynolds or turbulent stress. For a more general case of straight, steady uniform *3-D* open-channel flow, we have $\bar{u}_2$, $\bar{u}_3$, $\overline{u_1' u_2'}$, $\overline{u_2' u_3'} \neq 0$ in Equation (1.1), with the overall mass flux being still represented by the primary velocity $\bar{u}_1$ as the cross-sectionally averaged $\bar{u}_2$ and $\bar{u}_3$ are zero (i.e., there is no overall mass flux across the flow or in the vertical direction). For such an idealised 3-D mean open-channel flow, the velocity components $\bar{u}_2$ and $\bar{u}_3$ describe the helical water motions orthogonal to the primary flow and thus are often defined as helical secondary flow(s). For more complex flows in curved channels with irregular banks, the decomposition of the time-averaged water motion into primary flow and helical secondary flow(s) may not be as simple, since $\bar{u}_2$ and $\bar{u}_3$ can also include contributions from a variety of cross-flows which are not necessarily helical. This issue in relation to secondary flows at river confluences has been comprehensively discussed in Rhoads and Kenworthy (1998, 1999) and Lane *et al.* (1999, 2000), with practical field examples in Parsons *et al.* (2007) and Szupiany *et al.* (2009), among others..

The simplified versions of the time-averaged momentum Equation (1.1) have been extensively used for explanation of the origin and mechanics of secondary flows, and for their modelling (e.g., Gessner, 1973; Townsend, 1976; Demuren and Rodi (1984); Bradshaw 1987; Ikeda and Parker (1989);Rodi, 1993; Yang, 2005; Ikeda and McEwan (2009). It has been shown, for example, that it is likely that secondary flows in straight channels are generated by transverse pressure gradients resulting from the turbulence anisotropy or turbulence heterogeneity observed for normal turbulent stresses $\overline{u_2' u_2'}$ and $\overline{u_3' u_3'}$ (e.g., Townsend, 1976). However, Equation (1.1), when used alone, may lead to potential misinterpretation of the secondary flow mechanisms and thus should ideally be supplemented with other flow dynamics equations. Examples of such misinterpretation are given, e.g., in Hinze (1967) and Gessner (1973), and one of them is highlighted in Section 1.2.2 below.

1.2.2 Energy Balance of the Mean Flow

In 1967, Hinze suggested that energy-based considerations are more suitable for analysing the secondary flow mechanics compared to the momentum equation and vorticity Equation (Hinze, 1967). His elegant analysis was mainly based on the turbulent energy balance and will be briefly described in the next subsection. As an alternative to the turbulent energy balance, Gessner (1973) proposed considering the mean flow energy balance. He deduced that the transverse gradients of the Reynolds shear stresses $\overline{u'_1 u'_2}$ and $\overline{u'_1 u'_3}$ are mostly responsible for the generation of secondary flows along channel corners, while the effects of the normal stresses $\overline{u'_2 u'_2}$ and $\overline{u'_3 u'_3}$ and the shear stress $\overline{u'_2 u'_3}$, highlighted by other researchers based on the momentum and vorticity equations, are of secondary importance. This conclusion, however, seems not to be universal, as follow-up analyses supported earlier findings about the significance of the normal stresses $\overline{u'_2 u'_2}$ and $\overline{u'_3 u'_3}$ (e.g., Demuren and Rodi (1984)). More recently, Yang and Lim (1997) used the mean flow energy balance to hypothesize that the surplus mean energy in any arbitrary flow volume will be transferred along the direction towards the nearest boundary. They applied this assumption to study the bed shear stress distribution in the presence of the secondary currents in uniform straight channels.

The potential of the mean energy balance for studying secondary flows is high and needs to be better explored. Below we propose an approach to how the mean energy balance can be utilized to look at possible energy fluxes between primary mean flow, secondary mean flow, and turbulence. The balance of the total mean kinetic energy (MKE) for an open-channel flow (and also for conduits/ducts) can be expressed as:

$$\underbrace{\frac{\partial}{\partial t}\left(\frac{\bar{u}_i^2}{2}\right) + \bar{u}_j \frac{\partial}{\partial x_j}\left(\frac{\bar{u}_i^2}{2}\right)}_{\text{rate of change of MKE}} = \underbrace{g_i \bar{u}_i}_{\text{energy income from gravity}} - \frac{\partial}{\partial x_j}\Bigg[\underbrace{\frac{1}{\rho}\bar{u}_i \bar{p}}_{\text{pressure transport}} + \underbrace{\bar{u}_i \overline{u'_i u'_j}}_{\text{turbulent transport}} - \underbrace{\nu \frac{\partial}{\partial x_j}\left(\frac{\bar{u}_i^2}{2}\right)}_{\text{viscous transport}}\Bigg] + \underbrace{\overline{u'_i u'_j}\frac{\partial \bar{u}_i}{\partial x_j}}_{\text{energy transfer between mean flow and turbulence}} - \underbrace{\nu\left(\frac{\partial \bar{u}_i}{\partial x_j}\right)^2}_{\text{dissipation of mean flow energy}} \tag{1.2}$$

This equation follows from the multiplication of Equation (1.1) by $\bar{u}_i$ and from some re-arrangements (e.g., Tennekes and Lumley, 1972). As already mentioned, simplified forms of Equation (1.2) have been used in Gessner (1973) and Yang and Lim (1997). However, for studying energy exchanges between the primary and secondary flows it is beneficial to decompose Equation (1.2) for the total MKE into two separate equations, i.e., for the primary flow MKE and for the secondary flow MKE. The first equation specifies the energy balance for the longitudinal velocity $\bar{u}_1$, while the second equation gives the combined energy balance for $\bar{u}_2$ and $\bar{u}_3$ (Equations (1.3) and (1.4), respectively):

$$\frac{\partial}{\partial t}\left(\frac{\bar{u}_1^2}{2}\right)+\bar{u}_j\frac{\partial}{\partial x_j}\left(\frac{\bar{u}_1^2}{2}\right)=g_1\bar{u}_1-\bar{u}_1\frac{1}{\rho}\frac{\partial\bar{p}}{\partial x_1}-\frac{\partial\bar{u}_1\overline{u'_1u'_j}}{\partial x_j}$$
$$+\nu\frac{\partial}{\partial x_j}\left(\frac{\partial}{\partial x_j}\frac{\bar{u}_1^2}{2}\right)+\overline{u'_1u'_j}\frac{\partial\bar{u}_1}{\partial x_j}-\nu\left(\frac{\partial\bar{u}_1}{\partial x_j}\right)^2 \qquad (1.3)$$

$$\frac{\partial}{\partial t}\frac{(\bar{u}_2^2+\bar{u}_3^2)}{2}+\bar{u}_j\frac{\partial}{\partial x_j}\frac{(\bar{u}_2^2+\bar{u}_3^2)}{2}=g_2\bar{u}_2+g_3\bar{u}_3$$
$$-\bar{u}_2\frac{1}{\rho}\frac{\partial\bar{p}}{\partial x_2}-\bar{u}_3\frac{1}{\rho}\frac{\partial\bar{p}}{\partial x_3}$$

$$-\frac{\partial\bar{u}_2\overline{u'_2u'_j}}{\partial x_j}-\frac{\partial\bar{u}_3\overline{u'_3u'_j}}{\partial x_j}+\nu\frac{\partial}{\partial x_j}\left(\frac{\partial}{\partial x_j}\frac{(\bar{u}_2{}^2+\bar{u}_3{}^2)}{2}\right)$$
$$+\overline{u'_2u'_j}\frac{\partial\bar{u}_2}{\partial x_j}+\overline{u'_3u'_j}\frac{\partial\bar{u}_3}{\partial x_j}-\nu\left(\frac{\partial\bar{u}_2}{\partial x_j}\right)^2-\nu\left(\frac{\partial\bar{u}_3}{\partial x_j}\right)^2 \qquad (1.4)$$

Applying Equations (1.3) and (1.4) for steady, uniform (straight) open-channel flow, $(\partial/\partial t=\partial p/\partial x_2=\partial/\partial x_1=0)$ with $g_1=g\sin\alpha\approx gS$, $g_2=0$, $g_3=-g\cos\alpha\approx-g$, and assuming the hydrostatic pressure distribution (i.e., $\rho g\cos\alpha+\partial\bar{p}/\partial x_3\approx0$), we obtain:

$$\bar{u}_2\frac{\partial}{\partial x_2}\left(\frac{\bar{u}_1^2}{2}\right)+\bar{u}_3\frac{\partial}{\partial x_3}\left(\frac{\bar{u}_1^2}{2}\right)=gS\bar{u}_1$$
$$-\left(\frac{\partial\bar{u}_1\overline{u'_1u'_2}}{\partial x_2}+\frac{\partial\bar{u}_1\overline{u'_1u'_3}}{\partial x_3}\right)+\left(\overline{u'_1u'_2}\frac{\partial\bar{u}_1}{\partial x_2}+\overline{u'_1u'_3}\frac{\partial\bar{u}_1}{\partial x_3}\right)$$
$$+VT_1+VD_1 \qquad (1.5)$$

$$\bar{u}_2\frac{\partial}{\partial x_2}\frac{1}{2}\left(\bar{u}_2^2+\bar{u}_3^2\right)+\bar{u}_3\frac{\partial}{\partial x_3}\frac{1}{2}\left(\bar{u}_2^2+\bar{u}_3^2\right)$$
$$=-\left(\frac{\partial\bar{u}_2\overline{u'_2u'_2}}{\partial x_2}+\frac{\partial\bar{u}_2\overline{u'_2u'_3}}{\partial x_3}\right)-\left(\frac{\partial\bar{u}_3\overline{u'_3u'_2}}{\partial x_2}+\frac{\partial\bar{u}_3\overline{u'_3u'_3}}{\partial x_3}\right)$$
$$+\left(\overline{u'_2u'_2}\frac{\partial\bar{u}_2}{\partial x_2}+\overline{u'_2u'_3}\frac{\partial\bar{u}_2}{\partial x_3}\right)+\left(\overline{u'_3u'_2}\frac{\partial\bar{u}_3}{\partial x_2}+\overline{u'_3u'_3}\frac{\partial\bar{u}_3}{\partial x_3}\right)$$
$$+VT_{2,3}+VD_{2,3} \qquad (1.6)$$

where viscous transport terms VT_1 and $VT_{2,3}$, and viscous dissipation terms VD_1 and $VD_{2,3}$ are:

$$VT_1=\nu\frac{\partial}{\partial x_2}\left(\frac{\partial}{\partial x_2}\frac{\bar{u}_1{}^2}{2}\right)+\nu\frac{\partial}{\partial x_3}\left(\frac{\partial}{\partial x_3}\frac{\bar{u}_1{}^2}{2}\right),$$
$$VT_{2,3}=\nu\frac{\partial}{\partial x_2}\left(\frac{\partial}{\partial x_2}\frac{(\bar{u}_2{}^2+\bar{u}_3{}^2)}{2}\right)+\nu\frac{\partial}{\partial x_3}\left(\frac{\partial}{\partial x_3}\frac{(\bar{u}_2{}^2+\bar{u}_3{}^2)}{2}\right)$$
$$VD_1=-\nu\left(\frac{\partial\bar{u}_1}{\partial x_2}\right)^2-\nu\left(\frac{\partial\bar{u}_1}{\partial x_3}\right)^2,$$
$$VD_{2,3}=-\nu\left(\frac{\partial\bar{u}_2}{\partial x_2}\right)^2-\nu\left(\frac{\partial\bar{u}_2}{\partial x_3}\right)^2-\nu\left(\frac{\partial\bar{u}_3}{\partial x_2}\right)^2-\nu\left(\frac{\partial\bar{u}_3}{\partial x_3}\right)^2$$

Equation (1.5) for the primary flow MKE and Equation (1.6) for the secondary flow MKE suggest that the following energy exchanges are likely to occur:

(1) For steady uniform (straight) open-channel flow, the external energy (i.e., potential gravity energy) is "pumped" into the mean kinetic energy of the primary flow only (term $gS\bar{u}_1$). This energy is then spatially redistributed by molecular and turbulent stresses, partly transferred to the turbulent kinetic energy, and partly dissipated into heat.

(2) The mean kinetic energy balance of the secondary flow Equation (1.6) does not explicitly include an external energy source, suggesting that the secondary flow should be fed only through coupling with the primary mean flow and/or turbulence. Equations (1.5) and (1.6) show that this coupling may occur through turbulent stresses $\overline{u'_1u'_2}$ and $\overline{u'_1u'_3}$ in (1.5) and $\overline{u'_2u'_3}$ in (1.6), as they have common velocity components between them and are involved in turbulent transport terms and in energy transfer between mean flow and turbulence (i.e., terms $\overline{u'_iu'_j}\partial\bar{u}_i/\partial x_j$). The latter terms are most probable candidates for the energy coupling between the primary and secondary flows as the transport terms $\partial\bar{u}_i\overline{u'_iu'_j}/\partial x_j$ in Equation (1.6) have to redistribute the already available energy of $\bar{u}_2$ and $\bar{u}_3$.

(3) Based on Equations (1.5) and (1.6) and some 3-D turbulence data (e.g., Nikora *et al.*, 1998), the following energy pathway may be suggested: (i) the mean primary flow (PF) is fed by gravity through $gS\bar{u}_1$; (ii) PF transfers part of the received gravity energy to turbulent kinetic energy (TKE); (iii) TKE feeds mean secondary flow (SF) energy in particular flow regions through a subset of $-\overline{u'_iu'_j}\partial\bar{u}_i/\partial x_j$; and (iv) SF returns part of the received kinetic energy back to turbulence in particular flow regions through a different subset of $-\overline{u'_iu'_j}\partial\bar{u}_i/\partial x_j$. In other words, this analysis suggests that turbulence serves, very likely, as an energy link between the primary mean flow and secondary mean flow(s). Specifically, this link may occur through helical coherent structures and/or near-bed bursting processes (see Section 1.3 for more discussion).

To elaborate the proposed considerations for specific flow scenarios one would need detailed turbulence measurements involving estimates of velocity derivatives. This task will soon be realistic, even for field experiments.

Another interesting example of how the MKE balance may help in better understanding of secondary flows can also be derived from Equation (1.2), considering this time the total MKE balance. For steady uniform flow we may assume that there is a region in a flow where the combined effect of the transport terms and viscous dissipation in Equation (1.2) may be neglected, leading to:

$$\bar{u}_2 \frac{\partial}{\partial x_2}\left(\frac{\bar{u}_i^2}{2}\right) + \bar{u}_3 \frac{\partial}{\partial x_3}\left(\frac{\bar{u}_i^2}{2}\right) \approx gS\bar{u}_1 + \overline{u'_i u'_2}\frac{\partial \bar{u}_i}{\partial x_2} + \overline{u'_i u'_3}\frac{\partial \bar{u}_i}{\partial x_3} \tag{1.7}$$

Equation (1.7) explicitly shows that the secondary flows may be generated in flow regions with a significant imbalance between the energy income $gS\bar{u}_1$ and the energy loss $\overline{u'_i u'_j}\,\partial\bar{u}_i/\partial x_j$ (for turbulence generation), that provides a mechanism for the mean energy re-distribution. As in the previous example, however, this speculation requires support from data. Similar considerations can also be instrumental for flows in curved channels.

1.2.3 Turbulent Energy Balance

Another way to look at the inter-relations between the primary and secondary flows is to use the budget of the turbulent kinetic energy (TKE):

$$\underbrace{\frac{\partial}{\partial t}\frac{\overline{u'_i u'_i}}{2}}_{\substack{\text{rate of}\\ \text{change}\\ \text{of TKE}}} + \underbrace{\bar{u}_j \frac{\partial}{\partial x_j}\frac{\overline{u'_i u'_i}}{2}}_{\substack{\text{convection of}\\ \text{TKE by mean}\\ \text{flow}}} = \underbrace{-\overline{u'_i u'_j}\frac{\partial \bar{u}_i}{\partial x_j}}_{\substack{\text{energy transfer}\\ \text{between mean flow}\\ \text{and turbulence}}} \underbrace{-\frac{\partial}{\partial x_j}\left[\frac{1}{\rho}\overline{p'u'_j}\right]}_{\substack{\text{pressure}\\ \text{transport}}} + \underbrace{\frac{\overline{u'_i u'_i u'_j}}{2}}_{\substack{\text{turbulent}\\ \text{transport}}} \underbrace{-\overline{\nu u'_i\left(\frac{\partial u'_i}{\partial x_j}+\frac{\partial u'_j}{\partial x_i}\right)}}_{\substack{\text{viscous}\\ \text{transport}}} \underbrace{-\frac{\nu}{2}\sum_{i,j}\overline{\left(\frac{\partial u'_i}{\partial x_j}+\frac{\partial u'_j}{\partial x_i}\right)^2}}_{\substack{\text{dissipation of}\\ \text{turbulent energy}}} \tag{1.8}$$

Equation (1.8) can be derived in a number of ways. For example, multiplying the Navier–Stokes equation by u_i, presenting u_i and p as $u_i = \bar{u}_i + u'_i$ and $p = \bar{p} + p'$, and then averaging, one may obtain the full kinetic energy equation. Subtraction of Equation (1.2) for MKE from this full equation will produce Equation (1.8) for TKE. Based on the available data for pipes, Hinze, 1967 suggested that for the flow regions away from the walls and the pipe centre, Equation (1.8) can be simplified, applying the boundary layer approximation, as:

$$\bar{u}_2 \frac{\partial}{\partial x_2}\frac{\overline{u'_i u'_i}}{2} + \bar{u}_3 \frac{\partial}{\partial x_3}\frac{\overline{u'_i u'_i}}{2} \approx -\overline{u'_1 u'_2}\frac{\partial \bar{u}_1}{\partial x_2} - \overline{u'_1 u'_3}\frac{\partial \bar{u}_1}{\partial x_3} - \frac{\nu}{2}\sum_{i,j}\overline{\left(\frac{\partial u'_i}{\partial x_j}+\frac{\partial u'_j}{\partial x_i}\right)^2} \tag{1.9}$$

Hinze (1967) concluded that Equation (1.9) implies the following general rule: "when in a localised region, the production of turbulence energy is much greater (smaller) than the viscous dissipation, there must be a transport of turbulence-poor fluid into (out of) this region and a transport of turbulence-rich fluid outwards (into) the region." This rule is well supported by observations of the secondary flows formed at channel corners and at bed roughness transitions (Hinze, 1973). It is easy to see that Equation (1.7) proposed in the previous subsection has been inspired by Hinze's Equation (1.9). Summing up these two equations together we can obtain an equation for the simplified balance of the total kinetic energy, i.e.:

$$\bar{u}_2 \frac{\partial}{\partial x_2}\left(\frac{\bar{u}_i^2 + \overline{u'_i u'_i}}{2}\right) + \bar{u}_3 \frac{\partial}{\partial x_3}\left(\frac{\bar{u}_i^2 + \overline{u'_i u'_i}}{2}\right) \approx gS\bar{u}_1 - \frac{\nu}{2}\sum_{i,j}\overline{\left(\frac{\partial u'_i}{\partial x_j}+\frac{\partial u'_j}{\partial x_i}\right)^2} \tag{1.10}$$

Equation (1.10) highlights a potentially more general rule for gravity-driven open-channel flows, i.e., the secondary flows are generated as a response to an imbalance in some flow regions between the external energy supply to the mean flow and the energy dissipation (viscous dissipation of the mean flow is neglected in Equations (1.7) and (1.10) as, in most cases, it is much smaller than the turbulent dissipation).

Equations (1.9) and (1.10) mainly relate to flows in straight channels. Detailed experimental analyses of the turbulent energy budget for secondary flows in a meandering channel have been reported in Blanckaert and de Vriend (2004, 2005a, 2005b). In their considerations, the authors combined the vorticity equation and the turbulent energy balance equation and showed that turbulence plays a minor role in the generation of the centre-region cell, which is mainly due to the centrifugal force. Another important observation made by these authors is that there are extensive flow regions within a channel bend where turbulent energy is transferred to the mean flow, playing a significant role in maintaining the outer-bank circulation cell. This observation provides some support to a suggested chain of energy transformations in an open-channel flow described in the previous subsection. The results of these authors will be considered in more detail in Section 1.3.

1.2.4 Mean Vorticity Equation

The idea of explaining the secondary flows in open channels using the mean vorticity equation was proposed by Einstein and Li (1958). The vorticity equation can be obtained by taking the curl of the momentum Equation (1.1) (or by its cross-differentiation). Einstein and Li (1958) focused on an equation for the streamwise vorticity component $\bar{\omega}_1$ that in the absence of the density stratification, and neglecting the Coriolis effect, can be expressed as:

$$\underbrace{\frac{\partial\bar{\omega}_1}{\partial t}}_{\substack{\text{rate of}\\ \text{change}}} + \underbrace{\bar{u}_j\frac{\partial\bar{\omega}_1}{\partial x_j}}_{\substack{\text{convection}\\ \text{by mean}\\ \text{flow}}} = \underbrace{\bar{\omega}_j\frac{\partial\bar{u}_1}{\partial x_j}}_{\substack{\text{vortex}\\ \text{stretching}\\ \text{and tilting}}} + \underbrace{\frac{\partial^2}{\partial x_2\partial x_3}\left(\overline{u'_3{}^2}-\overline{u'_2{}^2}\right)}_{\substack{\text{stress-related}\\ \text{vorticity}\\ \text{"generation"}}} + \underbrace{\left(\frac{\partial^2}{\partial x_3{}^2}-\frac{\partial^2}{\partial x_2{}^2}\right)\left(-\overline{u'_3u'_2}\right)}_{\substack{\text{stress}-\text{related}\\ \text{vorticity}\\ \text{"dissipation"}}} + \underbrace{\frac{\partial}{\partial x_j}\left(\nu\frac{\partial\bar{\omega}_1}{\partial x_j}\right)}_{\substack{\text{viscous "dissipation"}\\ \text{of mean vorticity}}} + \underbrace{\frac{\partial}{\partial x_1}\left(\frac{\partial-\overline{u'_1u'_2}}{\partial x_3}-\frac{\partial-\overline{u'_1u'_3}}{\partial x_2}\right)}_{\substack{\text{vorticity change due}\\ \text{to non-uniformity}}} \tag{1.11}$$

where the components of the mean vorticity vector $\bar{\omega}_j$ are defined as:

$$\bar{\omega}_1=\frac{\partial\bar{u}_3}{\partial x_2}-\frac{\partial\bar{u}_2}{\partial x_3},\ \bar{\omega}_2=\frac{\partial\bar{u}_1}{\partial x_3}-\frac{\partial\bar{u}_3}{\partial x_1},\ \bar{\omega}_3=\frac{\partial\bar{u}_2}{\partial x_1}-\frac{\partial\bar{u}_1}{\partial x_2}$$

Nezu (2005) used Equation (1.11) as a basis for subdivision of secondary flows into Prandtl's first and second kinds. In flow configurations when the vortex stretching and tilting term in (1.11) is dominant, the first kind of secondary current is observed as, for example, in meandering channels. With channel curvature tending to zero (straight channels) this term disappears, as can be explicitly seen in the vorticity equation written in natural coordinates (Blanckaert and de Vriend, 2004). The second kind of secondary current occurs when turbulence terms in Equation (1.11) are dominant, i.e., due to turbulent stress anisotropy and heterogeneity. Of course, in real flow configurations superposition of both mechanisms has to be considered.

Nezu and Nakagawa (1993) reported a comprehensive study of Prandtl's second kind of secondary flows in straight channels, based on a simplified version of Equation (1.11) for steady, uniform open-channel flow:

$$\bar{u}_2\frac{\partial\bar{\omega}_1}{\partial x_2}+\bar{u}_3\frac{\partial\bar{\omega}_1}{\partial x_3}=\frac{\partial^2}{\partial x_2\partial x_3}\left(\overline{u'_3{}^2}-\overline{u'_2{}^2}\right)+\left(\frac{\partial^2}{\partial x_3{}^2}-\frac{\partial^2}{\partial x_2{}^2}\right)\left(-\overline{u'_3u'_2}\right)+\frac{\partial}{\partial x_j}\left(\nu\frac{\partial\bar{\omega}_1}{\partial x_j}\right) \tag{1.12}$$

They concluded that secondary currents are generated as a result of differences between the first RHS term in (1.12), which is a production term, and the second RHS term, representing vorticity "dissipation", i.e., damping. The last term in (1.12) is negligible except very close to the solid boundary. The 18-year-old text by Nezu and Nakagawa (1993) is still the most comprehensive work on Prandtl's second kind of secondary flows in straight open channels.

Interesting results for curved channels based on the vorticity equation in natural coordinates have been recently reported by Blanckaert and de Vriend (2004). Using high-quality laboratory data they performed a combined analysis of the terms of the vorticity equation and the turbulent energy balance. The revealed complex structure of the secondary flow and associated turbulence properties were explained by the interplay of the effects of the centrifugal force and spatial distribution of the turbulent stresses (see also Section 1.3).

Although after Demuren and Rodi's (1984) and Nezu and Nakagawa's (1993) studies vorticity-related considerations are mainly based on Equations (1.11) and (1.12) for streamwise vorticity, it is worth noting that Gessner (1973) pointed out that two other equations, for the transverse and vertical components of the vorticity vector, can be even more important for explaining and predicting the secondary flows. This view, however, has not been properly explored yet.

1.2.5 Mean and Turbulent Enstrophy Balance Equations

The momentum, energy, and vorticity equations, briefly discussed above, have mainly been used for studying time-averaged secondary flows (i.e., mean streamwise vorticity). However, the time-averaged secondary flows are most likely a manifestation of frequently occurring instantaneous helical motions. The involvement of the fluctuating vorticity can be clearly seen if we use an alternative form of the vorticity Equation (1.11), i.e.:

$$\frac{\partial\bar{\omega}_i}{\partial t}+\bar{u}_j\frac{\partial\bar{\omega}_i}{\partial x_j}=\bar{\omega}_j\frac{\partial\bar{u}_i}{\partial x_j}-\underbrace{\frac{\partial}{\partial x_j}\left(\overline{\omega'_iu'_j}-\overline{\omega'_ju'_i}\right)}_{\substack{\text{turbulent}\\ \text{convection}}}+\underbrace{\frac{\partial}{\partial x_j}\left(\nu\frac{\partial\bar{\omega}_i}{\partial x_j}\right)}_{\substack{\text{turbulent}\\ \text{stretching}}} \tag{1.13}$$

where the Reynolds decomposition is used, i.e., $\omega_i = \bar{\omega}_i + \omega'_i$. The second RHS term represents effects of anisotropy and spatial heterogeneity of turbulent stresses expressed through correlations of fluctuating vorticity and velocity components. The derivative $\partial\overline{\omega'_j u'_i}/\partial x_j$ represents the gain (or loss) of mean vorticity due to stretching/tilting of the fluctuating vorticity by fluctuating strain rates, while the term $\partial\overline{\omega'_i u'_j}/\partial x_j$ represents vorticity transport in the x_j direction (e.g., Tennekes and Lumley, 1972). Similar to the mean energy and turbulent energy, the coupling between the mean and fluctuating vorticities can be expressed using equations for ${\bar{\omega}_i}^2/2$ and $\overline{\omega'_i\omega'_i}/2$, which represent two components of the mean product $\overline{\omega_i\omega_i}/2 = {\bar{\omega}_i}^2/2 + \overline{\omega'_i\omega'_i}/2$, where $\omega_i\omega_i$ is known as enstrophy. Although there are some analogies between the MKE and mean enstrophy ${\bar{\omega}_i}^2/2$ (ME), and between the TKE and the turbulent enstrophy $\overline{\omega'_i\omega'_i}/2$ (TE), their physical nature is different, i.e., the enstrophy represents a measure of the density of the kinetic energy of helical motions rather than of all motions (e.g., Tsinober, 2009). As with Equation (1.2) for MKE, the mean enstrophy balance can be obtained by multiplying Equation (1.13) with $\bar{\omega}_i$, i.e.:

Equations (1.14) and (1.15) have been extensively studied in turbulence research with particular focus on their simplified versions for high-Reynolds-number flows with homogeneous turbulence. There have been no studies, to the writers' knowledge, involving these equations in the analysis of secondary flows. The main reason for this is probably the absence of experimental assessments of the terms of Equations (1.14) and (1.15). However, with recent advances in laboratory and field instrumentation it is quite likely that such experimental data will soon appear. In addition, recent progress in numerical simulation techniques and computing capabilities (e.g., Keylock *et al*., 2005; Lyn, 2008; Zeng *et al*., 2008; Constantinescu *et al*., 2009; van Balen *et al*., 2009; Stoesser *et al*., 2010) also encourages exploration of the potential of Equations (1.14) and (1.15) for studying secondary flows. Thus, the inclusion of the enstrophy balances in this review is justified, as it highlights a potentially fruitful theoretical framework for coupling mean and fluctuating vorticity fields, with the latter formed, most likely, by helical coherent structures. There may be several coupling mechanisms between these fields, with the gradient production term $\overline{u'_j\omega'_i}\,\partial\bar{\omega}_i/\partial x_j$ being the most obvious candidate as it is

$$\underbrace{\frac{\partial}{\partial t}\left(\frac{1}{2}{\bar{\omega}_i}^2\right)}_{\substack{\text{rate of}\\ \text{change}\\ \text{of ME}}} + \underbrace{\bar{u}_j\frac{\partial}{\partial x_j}\left(\frac{1}{2}{\bar{\omega}_i}^2\right)}_{\substack{\text{convection of}\\ \text{ME by mean}\\ \text{flow}}} = \underbrace{-\frac{\partial}{\partial x_j}\bar{\omega}_i\overline{\omega'_i u'_j}}_{\substack{\text{transport of ME}\\ \text{by velocity-vorticity}\\ \text{interactions}}} + \underbrace{\overline{\omega'_i u'_j}\frac{\partial\bar{\omega}_i}{\partial x_j}}_{\substack{\text{gradient}\\ \text{production}\\ \text{of ME}}} + \underbrace{\bar{\omega}_i\bar{\omega}_j S_{ij}}_{\substack{\text{ME}\\ \text{stretching}\\ \text{by mean strain}}} + \underbrace{\bar{\omega}_i\overline{\omega'_j\frac{\partial u'_i}{\partial x_j}}}_{\substack{\text{ME stretching}\\ \text{by turbulent}\\ \text{strain}}}$$

$$+ \underbrace{\nu\frac{\partial^2}{\partial x_j\partial x_j}\left(\frac{1}{2}{\bar{\omega}_i}^2\right)}_{\substack{\text{viscous}\\ \text{transport}}} - \underbrace{\nu\frac{\partial\bar{\omega}_i}{\partial x_j}\frac{\partial\bar{\omega}_i}{\partial x_j}}_{\substack{\text{dissipation of}\\ \text{mean enstrophy}}} \tag{1.14}$$

where $S_{ij} = 0.5(\partial\bar{u}_i/\partial x_j + \partial\bar{u}_j/\partial x_i)$. The procedure for deriving the turbulent enstrophy balance is identical to that for the TKE balance (1.8), i.e., it involves multiplication of the equation for ω'_i by ω'_i, and then subsequent time-(ensemble)-averaging (or, alternatively, subtraction of the mean enstrophy balance from the total enstrophy balance):

included in both Equations (1.14) and (1.15), similar to the TKE production term $\overline{u'_i u'_j}\,\partial\bar{u}_i/\partial x_j$ in Equations (1.2) and (1.8).

To summarise this brief overview of potential approaches for studying secondary flows, it should be noted that the recently achieved consensus among researchers is that there should be no preferred equation. Instead,

$$\underbrace{\frac{\partial}{\partial t}\left(\frac{\overline{\omega'_i\omega'_i}}{2}\right)}_{\substack{\text{rate of}\\ \text{change}\\ \text{of TE}}} + \underbrace{\bar{u}_j\frac{\partial}{\partial x_j}\left(\frac{\overline{\omega'_i\omega'_i}}{2}\right)}_{\substack{\text{convection of}\\ \text{TE by mean}\\ \text{flow}}} = \underbrace{-\overline{u'_j\omega'_i}\frac{\partial\bar{\omega}_i}{\partial x_j}}_{\substack{\text{gradient}\\ \text{production of TE}}} \underbrace{-\frac{\partial}{\partial x_j}\frac{\overline{u'_j\omega'_i\omega'_i}}{2}}_{\substack{\text{turbulent}\\ \text{transport}\\ \text{of TE}}} + \underbrace{\overline{\omega'_i\omega'_j\frac{\partial u'_i}{\partial x_j}}}_{\substack{\text{TE production}\\ \text{by turbulent}\\ \text{stretching}}} + \underbrace{\overline{\omega'_i\omega'_j}\frac{\partial\bar{u}_i}{\partial x_j}}_{\substack{\text{change}\\ \text{of TE by}\\ \text{mean strain}}} + \underbrace{\bar{\omega}_j\overline{\omega'_i\frac{\partial u'_i}{\partial x_j}}}_{\substack{\text{“mixed”}\\ \text{production}}}$$

$$\underbrace{\nu\frac{\partial^2}{\partial x_j\partial x_j}\left(\frac{\overline{\omega'_i\omega'_i}}{2}\right)}_{\text{viscous transport}} - \underbrace{\nu\overline{\frac{\partial\omega'_i}{\partial x_j}\frac{\partial\omega'_i}{\partial x_j}}}_{\text{viscous dissipation}} \tag{1.15}$$

better understanding and predictions can only be achieved on the basis of combined approaches.

1.3 SECONDARY CURRENTS AND TURBULENCE

Although the importance of inter-relations between secondary currents and turbulence has been recognized since the beginning of the last century, knowledge concerning these inter-relations remains patchy and there are still significant gaps in our understanding of how they actually depend on each other. There are several conceptual frameworks in studying turbulence that represent different facets of turbulence. The most advanced among them are the Reynolds-averaging framework, the coherent structures concept, and the eddy cascade concept. The existing knowledge within these three directions is mostly related to 2-D (in a time-averaged sense) open-channel flows. The effects of mean flow three-dimensionality and secondary currents on turbulence are less understood and have been mainly studied in terms of bulk turbulence characteristics, with the most systematic and comprehensive work conducted by Nezu and his group for rectangular open-channel flows, as reviewed in Nezu (2005), and by Knight and his group for compound channels, as reviewed in Knight *et al*. (2009a).

The knowledge of these effects in more complex flows is much less complete although recent publications demonstrate some significant advances in studying flows in meandering channels (e.g., Blanckaert and de Vriend, 2004, 2005a, 2005b; Odgaard and Abad, 2008; Abad and Garcia, 2009a, 2009b; Blanckaert, 2009, 2010; Knight *et al*., 2009a; Sanjou and Nezu, 2009; Gyr, 2010; Sukhodolov and Kaschtschejewa, 2010), riffle-pools (e.g., MacVicar and Roy, 2007a, 2007b), tidally- forced channels (e.g., Fong *et al*., 2009), channel expansion-contractions (Papanicolaou *et al*., 2007), at river confluences (e.g., Rhoads and Sukhodolov, 2001; Sukhodolov and Rhoads, 2001; Boyer *et al*., 2006), and even in the complex situations of ice-covered rivers (Ettema, 2008). However, the relations between coherent structures, eddy cascade, and secondary currents remain poorly understood. Recent findings related to these inter-relations are briefly summarized below.

Within the *Reynolds-averaging framework*, turbulence is expressed with bulk parameters arising in the Reynolds-averaged equations for momentum, energy, and/or vorticity. Examples include turbulent energy, Reynolds stresses, absolute and relative turbulence intensities, velocity–vorticity correlations, enstrophy, and higher-order statistical moments such as skewness and kurtosis. The Reynolds-averaged equations represent both turbulence and secondary currents and therefore they seem to be a suitable platform for studying inter-relations between them. In recent studies of secondary currents in straight open channels, the focus has been on flows over rough gravel beds, extending and complementing the well-established results of Nezu's group (Nezu, 2005) for smooth-bed open-channel flows. The major finding that has been independently reported by at least four groups is that secondary flow cells in rough-bed flows cover the whole channel cross-section evenly, even at width-to-depth ratios as high as 20 (Albayrak (2008); Rodriguez and Garcia, 2008; Belcher and Fox, 2009; Blanckaert *et al*. 2010). Figure 1.2 shows an example of the multicellular structures observed in an experiment with smooth side walls and a rough bed (Rodriguez and Garcia, 2008). This finding differs significantly from that for smooth-bed flows, where secondary currents disappear in the centre of the channel at aspect ratios larger than 5.

The most striking feature of the reported multicellular secondary currents is that their origin cannot be linked to sediment motion on the bed or to the transverse heterogeneity in bed roughness, as beds were not water-worked and no particle sorting or topographic variations were observed. Rodriguez and Garcia (2008) explain this phenomenon by the effect of the large gradient in roughness between the smooth glass walls and the gravel bed in their experiments, leading to an enhancement of near-wall cells and transverse transport of vorticity towards the centre of the channel. On the other hand, based on their extensive experiments in rectangular and trapezoidal channels Blanckaert *et al*. (2010) propose that the formation of secondary flow cells over the entre channel width is a result of hydrodynamic instability driven by near-bank secondary currents.

These observations can be supplemented with those of Cooper and Tait (2008) who reported the presence of high-speed longitudinal streaks in the time-averaged fields of streamwise velocity over water-worked gravel beds (no sediment motion was observed during the experiments). Interestingly, Cooper and Tait (2008) found no correlation between the time-averaged velocity streaks and bed topography, suggesting that their origin is not linked to variation in bed roughness or topography. Although the authors reject the presence of secondary currents as the possible explanation of the observed velocity streaks, their data are consistent with signatures of such currents and thus they should perhaps not be readily dismissed as the potential cause of the streaks.

Altogether, the results of these studies suggest that multicellular currents exhibit some form of self-organisation triggered by the pre-existing corner helical flows enhanced by bed roughness. Furthermore, Albayrak's (2008) study hints that the number of cells at a particular aspect ratio may depend on the properties of bed roughness. These observations shed new light on the old

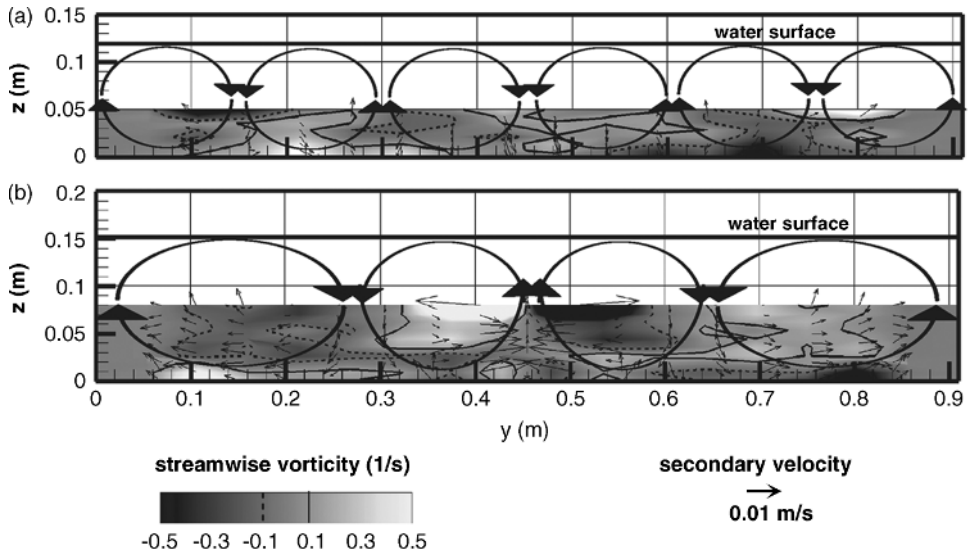

Figure 1.2 The results of a flume experiment with smooth walls and rough beds (Rodriguez and Garcia, 2008) at low flow (a) and high flow (b). The cells are delineated from the changes in direction in the streamwise vorticity and the directions of the secondary velocity. The cell size scales roughly with flow depth.

reports of longitudinal sediment ridges observed in some rivers (e.g., McLean, 1981; Nezu and Nakagawa, 1993) and may help in better formulations for channel morphodynamics. The physical origin of the observed multicellular structure is not yet clear and awaits a proper investigation.

Highlights of recent studies of the relation between secondary currents and turbulence in meandering channels include the detailed analysis of the spatial distribution of bulk turbulence properties by Blanckaert and de Vriend (2004, 2005a, 2005b). These authors performed comprehensive laboratory measurements of velocity vectors in a sharp open-channel bend, focusing on a bicellular pattern of secondary currents and its interrelations with turbulent energy, its production, dissipation, and transport. The revealed circulation pattern includes the classical centre-region helical cell and a weaker and smaller counter-rotating outer-bank cell (believed to play an important role in bank erosion processes). By analysing simultaneously the vorticity equation and the kinetic energy transfer between the mean flow and turbulence, the authors established that the centre-region cell is mainly formed due to the centrifugal force while the turbulence contribution is minor, as one could expect. The data also suggest that the origin of the outer cell can be explained by the interplay of the near-bank turbulence heterogeneity and channel curvature effects. This finding is somewhat consistent with laboratory and LES numerical studies of secondary circulation at the corners formed by a solid vertical wall and flow free surface, i.e., at mixed-boundary corners (e.g., Grega *et al*., 2002; Broglia *et al*., 2003). However, in straight channels the mixed-boundary (inner) corner vortex rotates toward the solid wall at the water surface while in a curved channel the vortex rotation is opposite, probably reflecting additional effects of the centrifugal force and the associated centre-region cell. Blanckaert and de Vriend (2005b) proposed that the observed significant deviation of the turbulence structure in a curved channel from its straight channel counterpart is due to the streamline curvature effects. The transverse "stratification" of bulk turbulence properties is explained using an analogy with buoyancy-induced stratification and, therefore, can be quantified with the "curvature-flux-Richardson" number. The recent LES-based numerical study of van Balen *et al*. (2009, 2010) reproduces all key features observed in the laboratory experiments, additionally emphasizing the enhanced TKE and its production in the region of the outer near-bank cell.

Blanckaert and de Vriend's (2004, 2005a, 2005b) experiments covered an idealized situation of an isolated bend where the effects of adjacent bends were not present. A more realistic channel shape was used in recent experiments by Abad and Garcia (2009a, 2009b) who performed extensive velocity measurements in a unique five-bends facility known as the "Kinoshita channel" and reported detailed maps of mean velocity vectors, Reynolds stresses, and TKE. Both fixed-bed and mobile-bed scenarios were examined, particularly focusing on the effects of bend orientation, i.e., upstream or

downstream. For a flat, smooth bed condition, the measurements revealed that at the bend apex the maximum velocity occurs near the inner bank for both upstream and downstream bend orientations. However, for the upstream-oriented bends, secondary flow was weaker compared to that in the downstream-oriented bends. Even more interesting, the hydraulic resistance factor appeared to depend on bend orientation, i.e., for the same channel sinuosity the resistance was higher for the downstream-skewed bends, probably reflecting stronger secondary currents. The laboratory data described above can be compared with comprehensive field turbulence measurements in a bend of the Spree River where the level of detail and measurement accuracy can compete with those in the laboratory set-ups (Sukhodolov and Kaschtschejewa, 2010). An example of a field study in a bend of the Tollense River near Lebbin (Germany) by Sukhodolov's group is shown in Figure 1.3.

These findings relate to the time-averaged structure and represent a significant step forward in our current understanding of secondary flows in straight and curved channels. However, the averaging procedures eliminate details on key agents forming this "time-averaged" structure. These agents are most likely coherent structures and eddy cascades, discussed below.

The concept of *coherent structures* is based on the recognition of some order in turbulence. A coherent structure (or eddy) can be broadly defined as a 3-D flow region over which at least one fundamental flow variable exhibits significant correlation with itself or with another variable over a range of space and/or time (e.g., Robinson, 1991; Roy *et al*., 2004; Adrian, 2007). Many kinds of coherent structures have been identified, depending on flow type and Reynolds number, and it has been shown that they play a significant role in mass and momentum transfer in rivers. The issue of identifying, detecting, and quantifying coherent structures remains a hot research topic in physics, engineering, and the earth sciences. It is likely that at least some secondary currents in river flows are formed by helical coherent structures, intermittently or quasi-periodically appearing in particular regions of the channel cross-sections (e.g., at corners). In addition (or independently), secondary flow cells can be partly controlled by the spatial distribution and intensity of near-bed bursting processes. These possibilities have been highlighted by works of Nakagawa and Nezu (1981), Gulliver and Halverson (1987), Nezu and Nakagawa (1993), Lane *et al*. (2000), Blankaert and de Vriend (2005b), Albayrak (2008), Sterling *et al*. (2008), Buffin-Bélanger *et al*. (2009), Miyawaki *et al*. (2009), and Pinelli *et al*. (2010). These mechanisms are also consistent with the analysis of the mean flow energy balance in Section 1.2.2, where it is proposed that secondary flows are fed by turbulence.

Pinelli *et al*. (2010) performed direct numerical simulations of smooth-wall turbulent flow in a straight square duct with a particular focus on the role of coherent structures in the generation and characterization of near-corner cells. They found that the buffer layer structures determine the distribution of mean streamwise vorticity, while the shape of the cells is influenced by larger-scale motions. Pinelli *et al*.'s (2010) paper is probably the first quantitative report that explicitly demonstrates close interconnections between near-corner secondary flows with both buffer-scale and duct-scale

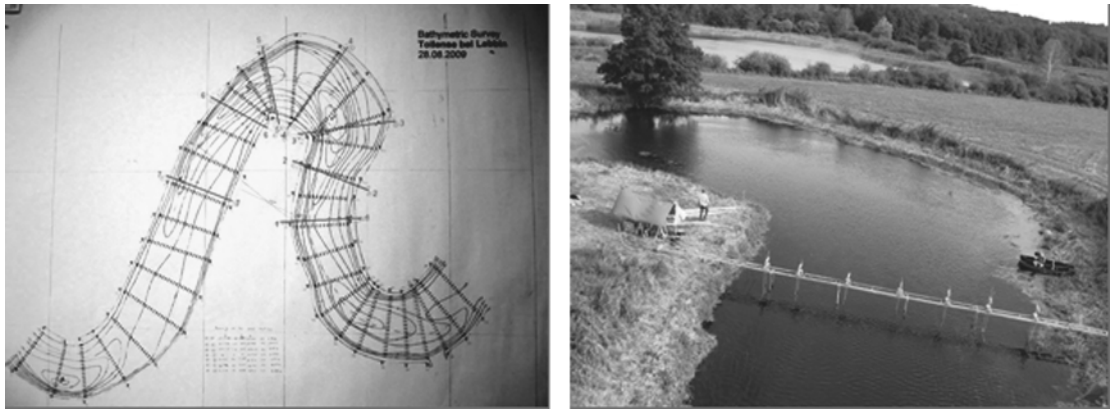

Figure 1.3 Field experimental set-up in a bend of the Tollense River near Lebbin (2009) for studying secondary currents by the research group of A. Sukhodolov, Leibniz-Institute of Freshwater Ecology and Inland Fisheries, Berlin, Germany.

coherent structures. Although the range of Reynolds numbers was quite limited and flow configuration was very simplified, this study highlights potentially important effects that may be directly relevant to river flows. More realistic conditions of open-channel gravel bed flow have been studied by Albayrak (2008). Based on extensive experiments in a large, straight, gravel bed flume, Albayrak (2008) explored properties of prevailing coherent structures and their relation to the secondary flow cells. He found that Adrian's (2007) model of hairpin packets is applicable to the conditions of rough-bed open-channel flows, confirming earlier findings of Hurther *et al*. (2007). Furthermore, Albayrak (2008) showed that the vertical extension of the hairpin packets is significantly enhanced in upwelling zones of the secondary flow cells and reduced in downwelling zones. Albayrak's (2008) data also suggest that the time-averaged secondary flow cells represent effects of large instantaneous helical structures, similar to those observed by Gulliver and Halverson (1987).

Turbulent structures in a channel bend with well-documented secondary flow cells and bulk turbulence parameters were studied by Blankaert and de Vriend (2005b). These authors showed, for the first time, that velocity fluctuations within a bend can be considered as a superposition of large-scale structures occupying the whole channel cross-section and small-scale "background" turbulence. Large-scale width-coherent velocity fluctuations resemble wavelike motions and mainly contribute to the normal turbulent stresses, while the "background" turbulence is a main contributor to the shear stress generation. The origin of these two components and interrelations between them need further investigation.

A more intricate case of a meandering compound open-channel flow was examined by Sanjou and Nezu (2009) who employed a multilayer scanning PIV and revealed a strong connection between the horizontal vortices and secondary currents. Their phenomenological model is summarized in Figure 1.4. Buffin-Bélanger *et al*. (2009) and Demers *et al*. (2011) considered an even more complicated case of an ice-covered meandering flow and addressed the question of how coherent structures rising from the bed and ice boundaries interact and modify the overall structure of the flow. Based on laboratory and field studies, they compared an ice-covered flow and an ice-free flow in the same channel. They discovered that the flow field in the ice-covered condition is characterized by two counter-rotating helical cells at the bend entrance which evolve, further downstream, into one helical cell that rotates in the opposite direction compared to that without the ice cover. Turbulence properties are also significantly different for these two scenarios, showing low correlations between

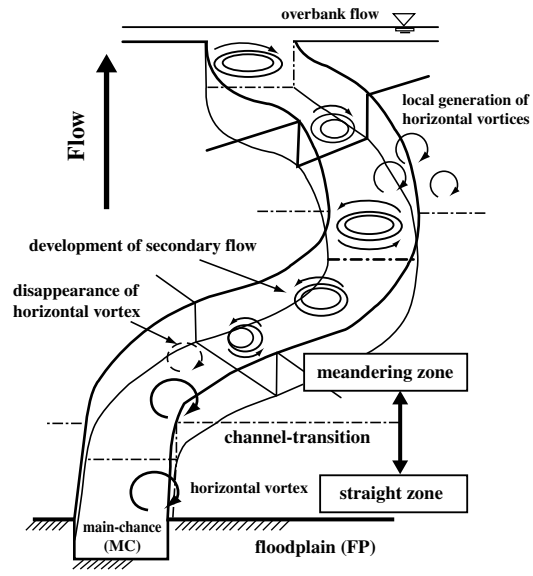

Figure 1.4 Phenomenological flow model of horizontal vortices and secondary currents in meandering compound open-channel flow (Sanjuo and Nezu, 2009).

structures generated at the bed and at the ice cover, as if the two boundary layers were disconnected. How exactly these structures influence secondary flow cells in this most complicated set-up remains unclear.

The *eddy cascade concept* reflects the multiscale structure of turbulence. According to this concept, turbulence is initiated at an external scale of the flow (e.g., flow depth or width in a stream) as a result of hydrodynamic instability that transfers the energy from an external forcing to the largest eddies comparable to the external flow scale. These large eddies being unstable themselves then transfer their energy to smaller eddies and so on, until the eddy size reaches the so-called dissipative scale. At this scale, viscous forces overcome inertial forces and turbulence becomes suppressed by viscosity. The key analyses of this approach include velocity spectra, correlations, and structure functions (e.g., Tennekes and Lumley, 1972). In time-averaged 2-D open-channel flow over a flat bed, the eddy cascade is assumed to start with generation of large eddies (2–5 flow depths H in length and 1–2 H in width), which then will cascade their energy down to the dissipative scale. In this scenario, there is only one external scale and associated energy supply to turbulence from the mean flow. In rivers, of course, there may be several superimposed mechanisms of TKE production associated with multiscale bed forms. Altogether they represent

different canals of energy transfer from the mean flow to turbulence (Nikora, 2008).

In addition to these mechanisms, the helical secondary flows may introduce a potentially important external scale and associated instability that may modify conventional transport of energy from gravity to the mean flow to the depth-scale eddies and through the eddy cascade to heat. Alternative scenarios are also possible. As has been highlighted in Section 1.2.2, it is quite likely that secondary flows in straight channels receive their energy from turbulence, suggesting the existence of an inverse energy cascade (i.e., flux of energy from smaller scales to larger scales to the mean flow) in particular regions of the flow. This conjecture is supported by Blanckaert and de Vriend's (2004) experiments. However, until now there have been no systematic studies of this aspect of secondary flow–turbulence interactions.

1.4 SECONDARY CURRENTS AND HYDRAULIC RESISTANCE

Although the effect of secondary currents on hydraulic resistance is widely recognized, its nature is not yet clear. Thus, its explicit incorporation into resistance equations is still an unsolved problem (e.g., Yen, 2002). In general, secondary currents modify the transverse distributions of mean velocities, fluid shear stresses, and bed shear stress. It is often assumed that these modifications increase the bulk friction factor $f = 8(u_*^2/U_o^2)$ compared to the case when secondary currents are absent ($u_*^2 = \tau_o/\rho$, U_o is cross-section mean velocity, τ_o is a "reach-scale" bed shear stress). There are also indications that in some situations secondary flows do not affect the bulk friction factor, while significantly altering boundary shear stress and near-bank velocities (Kean et al., 2009). Indeed, since the bulk friction factor $f = 8(u_*^2/U_o^2)$ is a result of integration of the Reynolds-averaged momentum equation over the whole cross-section (or even over a river reach), the different resistance mechanisms are lumped together, making it difficult to unambiguously observe their individual contributions.

A more practical approach to account for the presence of secondary currents is to use the depth-averaged momentum equation and the local friction factor $f = 8(\tau_b/\rho U_d^2)$ defined at a particular vertical at the transverse coordinate y, where $\tau_b(y)$ is a "local" bed shear stress, and $U_d(y)$ is the depth-averaged velocity. This approach has been extensively developed and explored by Knight and his group (Knight *et al*. 2009a, 2009b, and references therein). Their work provides a thorough theoretical analysis, in-depth experimental support, and implementation in a range of analytical and computer models. The conceptual basis of the approach is the depth-averaged momentum equation expressed as (Knight *et al*. 2009a):

$$\underset{\substack{\text{gravity}\\ \text{term}}}{\rho g H S} + \underset{\substack{\text{transverse}\\ \text{stress term}}}{\frac{\partial}{\partial y}(H\hat{\tau}_{yx})} - \underset{\substack{\text{local bed}\\ \text{shear stress}}}{\tau_b\left(1+\frac{1}{s^2}\right)^{1/2}} = \underset{\substack{\text{secondary}\\ \text{flow term}}}{\frac{\partial}{\partial y}(\rho H \bar{u}\bar{v})_d} \quad (1.16)$$

where H is the flow depth, $\hat{\tau}_{yx}$ is the depth-averaged transverse shear stress, s is the transverse bed slope (i.e., dz_b/dy), $\bar{u}$ and $\bar{v}$ are local time-averaged longitudinal and transverse velocities, and an index "d" in the secondary flow term indicates depth-averaging. The local friction factor $f = 8(\tau_b/\rho U_d^2)$ is involved in the parameterization of the transverse stress term and the bed shear stress term. Knight *et al*. (2009a) reviewed a range of closure models for the terms of Equation (1.16) and demonstrated their applicability for both straight and meandering compound channels, including those with vegetated floodplains. The reliability of the 2-D resistance models can be further strengthened if deeper understanding of the secondary flow mechanisms is developed and, based on this, more appropriate closures for the secondary flow term in Equation (1.16) are proposed (currently this term is often assumed to be a constant). The research in this direction is ongoing and can be well illustrated with recent results by Blanckaert (2009, and references therein), who proposed a set of relations describing different effects of secondary currents in meandering channels on the hydraulic resistance factor. The effect of bend orientation on hydraulic resistance, recently discovered by Abad and Garcia (2009a, 2009b) has already been mentioned in Section 1.3.

A potentially useful framework for assessment of secondary flow effects on hydraulic resistance has been recently suggested in Nikora (2009). Starting with the Reynolds-averaged momentum equation, he derived a relation for partitioning the bulk and local friction factors into constitutive components, accounting for the effects of: (i) viscous stress; (ii) turbulent stress; (iii) form-induced stress; (iv) flow unsteadiness and spatial heterogeneity of mean velocities (e.g., due to non-uniformity and/or secondary currents); (v) spatial heterogeneity of turbulence characteristics (e.g., due to secondary currents); and (vi) vertical heterogeneity of driving forces. These components of the friction factor account for the roughness geometry and highlight the significance of the Reynolds and form-induced stresses in the near-bed region, where their values are the largest. The suggested relation can guide better understanding of the resistance mechanisms and developing their parameterizations and models.

1.5 SECONDARY CURRENTS, SEDIMENTS AND MORPHODYNAMICS

Since the pioneering works of river navigation engineers, it is widely accepted that secondary flows play a significant role in channel deformation, bank stability, and sediment transport. One of the historically earliest explanations of secondary currents involved suspended sediments as a key factor of their generation (Vanoni, 1946). In his experiments, Vanoni (1946) noticed that the addition of a small amount of fine sediments in a clear-water open-channel flow led to the modification of the velocity distribution across the channel and formation of longitudinal streaks in the suspended sediment concentration field (three strong streaks at the channel centre and weaker streaks near the walls). Thus, Vanoni considered the effect of suspended sediment to be a cause of the observed secondary currents.

This experimentally guided conjecture was later replaced by the alternative idea that the observed suspended sediment streaks are generated by the pre-existing secondary currents. A recent study by Hallez and Magnaudet (2009), however, points out the possibility of generating secondary currents, even by weak density stratification, which could have been created in the Vanoni experiments by the addition of suspended sediments. In light of Hallez and Magnaudet's (2009) study, it is beneficial to reconsider Vanoni's (1946) abandoned hypothesis, which may well be correct, representing a specific form of Prandtl's second kind of secondary current.

The formation of sand ribbons on the beds of straight channels is another similar phenomenon that has been known for a long time and that is often explained by some kind of self-organization involving flow-bed sediment interactions (e.g., McLean, 1981; Nezu and Nakagawa, 1993; Garcia, 2008; Parker, 2008). Colombini (1993) and Colombini and Parker (1995) proposed an instability-based mechanistic explanation for these bed features, while McLelland *et al*. (1999) and Wang and Cheng (2006) provided the most systematic recent account on this topic, supported by extensive laboratory experiments with bimodal sediments and artificial bedforms.

Although bank erosion is often associated with secondary currents, detailed and reliable information on the mechanisms involved and their quantitative measures has become available only recently. Comprehensive reviews of various predictive engineering methods for bank erosion involving effects of secondary currents can be found in Pizzuto (2008) and Rinaldi and Darby (2008). These methods are often based on the depth-averaged Equation (1.16) and on parameterizations proposed by Knight and his group (e.g., Knight *et al*., 2009a). Among recent works, special attention should be given to Papanicolaou *et al*.'s (2007) study, which combined detailed turbulence measurements in a gravel-bed stream (with cohesive banks) with extensive laboratory erosion tests. The 3-D and depth-averaged momentum equations, similar to Equations (1.1) and (1.16), were used by the authors as a framework for data analysis and interpretation. Papanicolaou *et al*. (2007) demonstrated that secondary currents increase the magnitude of the depth-averaged sidewall shear stress by a factor of at least 2.0, while the ratio of the maximum to the depth-averaged sidewall shear stress was found to be larger than 5. This finding suggests that the conventional approaches in morphodynamics based on the depth-averaged sidewall shear stress may not be a suitable approximation of the reality for natural channels with complex morphology involving contractions and expansions.

Another highlight of the influence of secondary flows on sediment transport is a study of bend orientation (curvature) effects on sediment dynamics and, through this, on morphodynamics (Abad and Garcia, 2009b). This study is complementary to the already mentioned set of experiments in the same facility with a fixed bed (Abad and Garcia 2009a). The experiments with mobile beds revealed significant differences in sediment dynamics between upstream- and downstream-oriented bends. In particular, downstream-oriented bends generated stronger secondary currents and more distinct bed forms, with higher shear stresses along the bed and banks. These hydrodynamic features may have significant morphological effects as they most likely produce higher erosion power and enhanced sediment transport rates leading to increased channel migration rates. In addition, this study provides qualitative and quantitative information on potential effects of secondary currents and flow non-uniformity on dune shape, sizes, and migration rates, knowledge of which is still very limited (Best, 2005). Consideration of Abad and Garcia's (2009b) study should be supplemented with laboratory experiments of Termini (2009) and Jamieson *et al*. (2010), which expand a range of Abad and Garcia's (2009b) scenarios in terms of bend shape and hydraulic conditions.

The more complicated case of braided channels involves a wide spectrum of secondary flow patterns that are the inherent component of nearly all morphodynamic processes occurring in this highly dynamic channel type. Specific examples can be found in a recent specialized volume on braided channels edited by Sambrook Smith *et al*. (2006). Although there have been some important advances in this area (e.g., Ashworth, 1996; De Serres *et al*. 1999; Richardson and Thorne, 2001), knowledge of secondary flows in braided channels remains fragmentary and rather qualitative. Quickly developing simulation methodologies such as DNS (direct numerical simulation) and LES (large eddy simulation) may soon appear to be of great help by complementing laboratory and field studies

in clarifying details of secondary flows for typical elements of braided channel morphology such as confluences, bifurcations, islands, and anabranches (e.g., Keylock *et al*., 2005; Lyn, 2008; Zeng *et al*., 2010). A recent example of a successful application of the detached eddy simulation (DES) technique for studying flow structure at a river confluence is given in Miyawaki *et al*. (2009). This study convincingly shows that the time-averaged helical currents at the confluences are a result of frequently occurring helical coherent structures (Figure 1.5).

The most challenging scenarios for secondary currents and their roles in sediment transport and channel morphodynamics occur, not surprisingly, in ice-covered rivers. Due to the great technical difficulties of wintertime field work, the knowledge of secondary currents in ice-covered rivers is very fragmentary. Wide-ranging reviews of channel responses to ice cover are given in Ettema (2002, 2008), while unique data and their conceptualization are provided in Tsai and Ettema (1994), Ettema and Zabilansky (2004) and in the already discussed work of Buffin-Belanger *et al*. (2009) and Demers *et al*. (2011). Tsai and Ettema, 1994 studied the ice cover effect on the circulation pattern and its strength in a curved channel in a laboratory flume. The authors showed that the ice cover changes the topology of the secondary flow cells and dampens their strength. Ettema and Zabilansky (2004) reported unique wintertime fieldwork along the Fort Peck reach of the Missouri River. They documented, for the first time, how exactly ice cover can modify flow structures that trigger associated morphological responses, such as the migration of channel bends, transient scours, sediment deposition, and cyclic shifts of the thalweg through sinuous-braided subreaches. All these changes reflect changes in secondary flow patterns accompanied by many other superimposed changes due to the ice cover.

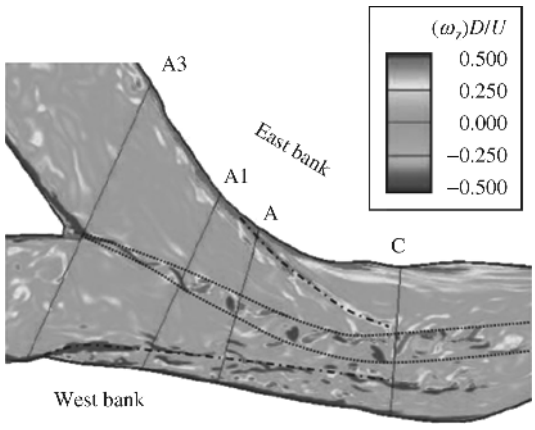

Figure 1.5 Instantaneous vorticity at the confluence visualized with the contours on the water surface (Miyawaki *et al*., 2009). (See color version of this figure in color plate section.)

1.6 SECONDARY CURRENTS AND MIXING PROCESSES

The presence of secondary currents may significantly modify vertical, transverse, and longitudinal mixing, as discussed in detail in Rutherford (1994). Depending on the specific flow configuration, secondary currents may either enhance or dampen mixing rates in all directions or selectively. For example, an increase in transverse mixing due to secondary currents may be associated with a reduction in longitudinal mixing. Progress in understanding the mixing processes when secondary currents are present depends on the depth of understanding of the overall hydrodynamics of secondary currents and of their inter-relations with turbulence.

In relation to straight channels, secondary flow effects on mixing in rectangular and one-sided compound channels have recently been considered by Kang and Choi (2009). Using the injection of dye into the compound channel, these authors found that the secondary flow cells move the location of the maximum dye concentration towards the floodplain, leading to a skewed distribution of the mean dye concentration in the spanwise direction. A similar but weaker effect was noted for rectangular channels. Kang and Choi (2009) also showed that the Reynolds fluxes reduce the concentration peak and thicken the tails of the mean dye concentration, while secondary currents affect the magnitude of the mean concentration over the entire channel width, moving the peak concentration in the flow direction.

These results can be supplemented with earlier experimental data obtained in a straight, smooth-bed channel that highlight particular features in the flow regions around the local symmetry z–x planes between the helical secondary currents near side-walls and the central part of the flow (Nikora *et al*., 1998). These regions are characterized by some anomalous properties:

(1) Local minima in the longitudinal velocity which coincide with the local maxima in the vertical velocity, i.e., the minima in the longitudinal velocity occur in the upflow regions where the transverse velocity changes its sign.
(2) Local minima in the transverse eddy diffusivity and in the turbulent energy generation term $-\overline{u'v'}\,d\bar{u}/dy$, surrounded by local maxima in these variables.
(3) The transverse turbulent flux $-\overline{u'v'}$ in the near-bed layer is close to zero and changes its sign from

minus to plus (this means that transverse turbulent fluxes occur towards the boundary between each helical secondary current and the central flow).

(4) Fluid ejections are suppressed while fluid sweeps are increased, in agreement with the transverse distributions of velocity skewness and kurtosis.

Thus, the data suggest the existence of an interesting phenomenon – the suppression of transverse mixing in the narrow regions between the helical near-wall currents and the central flow. A qualitative confirmation of the suggested phenomenon can be found in aerial photographs from tracer experiments depicted on the cover of Rutherford's (1994) book. They clearly show suppressed mixing between stable dye strips near the banks and the central flow of the Waikato River in New Zealand. This could be explained by the near-bank helical currents, which suppress mixing between the near-bank flow region and the central flow region. However, this effect requires further investigation for a wider range of conditions.

In relation to curved channels, recent research on the effects of the mechanics of secondary flows on mixing processes has been reported by Boxall *et al*. (2003) and Marion and Zaramella (2006) for large laboratory self-formed channels, and by Rowinski *et al*. (2008) for the field sites. These authors show that channel curvature may have two effects on dispersion that tend to oppose each other. On one hand, curvature increases the longitudinal dispersion, reflecting an increase in the turbulence intensity. On the other hand, it reduces dispersion by enhancing transverse mixing. These results also show that the most efficient longitudinal dispersion occurs at the bend entrance, sharply decreasing beyond the meander apex. Theoretical and modelling aspects of the secondary flow effects on mixing and dispersion processes have been recently addressed by Czernuszenko and Rylov (2002), Albers and Steffler (2007), and Khosronejad *et al*. (2007), among others.

1.7 CONCLUSIONS

Twenty three years ago Bradshaw (1987) concluded that "Flows with strong skew-induced streamwise vorticity or flows dominated by stress-induced vorticity are particularly challenging, and the main conclusion of the present review is that we lack basic physical understanding of the effect of mean-flow three dimensionality on turbulence structure." His closing words were: "The step from 2-D to 3-D mean flow is as difficult in simulation as in experiment. . ." (Bradshaw 1987). Today, these conclusions remain largely valid, especially in relation to gravel bed rivers, where a complex combination of multiscale secondary currents is an inherent feature.

The present review shows that, although significant recent advances should be acknowledged in understanding the secondary flow mechanics and their inter-relations with other river processes, there are still many knowledge gaps that have to be addressed. In particular, these gaps relate to quantification and prediction of secondary flow effects on sediment transport, hydraulic resistance, mixing, and morphodynamics. Furthermore, the researcher's attention should be also extended to the identification of the role of secondary currents in the functioning of stream ecosystems. The profound effect of secondary currents on the mean velocities, turbulence, mixing, and sediment dynamics is likely to be reflected in ecosystem structure and functioning, but this effect remains to be understood and quantified. This focus area highlights the significance of secondary flows from a multidisciplinary perspective.

To achieve the goal of greater understanding, a number of theoretical, experimental, and conceptual issues should be resolved. In relation to theoretical analyses, a conceptual uncertainty related to the cause-and-effect relations between key processes and variables awaits to be resolved. This can only be achieved on the basis of combined approaches involving various forms of the Navier–Stokes equations, from the RANS to the enstrophy equations. There are also methodological issues that require urgent attention, with identification and quantification of secondary flow patterns in complex flows being among the most challenging. This task is particularly relevant to secondary flows in braided channels where partitioning into primary and secondary flows is, in most cases, unclear. The solution may be sought using analogies with the problem of coherent structure identification in turbulent flows, where a variety of invariant measures (i.e., independent of the coordinate system orientation) have been explored. Progress in this direction should advance the topological and mechanistic classification of secondary currents in river flows that, once developed, should help in a better coupling between channel morphology, flow structure, and sediment dynamics at multiple scales. In relation to the data base, laboratory studies, and quickly developing numerical simulation techniques need to be complemented by comprehensive field studies. Work in this direction is growing (e.g., Sukhodolov and Rhoads, 2001; Rhoads and Sukhodolov, 2001; Ettema and Zabilansky, 2004; Buffin-Belanger *et al*. 2009; Fong *et al*. 2009; Rowinski *et al*., 2008; Sukhodolov and Kaschtschejewa, 2010).

1.8 ACKNOWLEDGEMENTS

VN acknowledges support from the Engineering and Physical Sciences Research Council, UK, Grant EP/G056404/1 "High resolution numerical and experimen-

tal studies of turbulence-induced sediment erosion and near-bed transport" and from the Leverhulme Trust, UK, Grant F/00152/Z "Biophysics of flow-plants interactions in aquatic systems". AGR acknowledges financial support from the Natural Sciences and Engineering Research Council of Canada and the Canada Research Chair program. K. Blanckaert, G. Constantinescu, S. Cameron, N. Nikora, and M. Stewart provided useful comments on earlier versions of the manuscript. Reviews by Bruce MacVicar and Thanos Papanicolaou helped to sharpen the focus of this paper.

1.9 REFERENCES

Abad, J.D. and Garcia M.H. 2009a. Experiments in a high-amplitude Kinoshita meandering channel: 1. Implications of bend orientation on mean and turbulent flow structure. *Water Resources Research* **45**: W02401. doi:10.1029/2008 WR007016.

Abad, J.D. and Garcia M.H. 2009b. Experiments in a high amplitude Kinoshita meandering channel: 2. Implications of bend orientation on bed morphodynamics. *Water Resources Research* **45**: W02402. doi:10. 1029/2008 WR007017.

Adrian R.J. 2007. Hairpin vortex organization in wall turbulence. *Physics of Fluids* **19**: 041301.

Albayrak, I. 2008. *An experimental study of coherent structures, secondary currents and surface boils and their interrelation in open-channel flow*. Ph.D. Thesis, École Polytechnique Fédérale de Lausanne, no. 4112: 281pp. doi: 10. 5075/epfl-thesis- 4112.

Albers, C. and Steffler, P. 2007. Estimating transverse mixing in open channels due to secondary current-induced shear dispersion. *Journal of Hydraulic Engineering* **133**: 186–196.

Ashworth, P.J. 1996. Mid-Channel bar growth and its relationship to local flow strength and direction. *Earth Surface Processes and Landforms* **17**: 103–124.

Belcher, B.J. and Fox, J.F. 2009. Discussion of "Laboratory measurements of 3-D flow patterns and turbulence in straight open channel with rough bed" by Rodriguez, J.F. and Garcia, M. H. *Journal of Hydraulic Research* **47**: 685–688.

Best, J. 2005. The fluid dynamics of river dunes: A review and some future research directions. *Journal of Geophysical Research – Earth Surface* **110**: F04S02. doi: 10.1029/2004JF000218.

Blanckaert, K. 2009. Saturation of curvature induced secondary flow, energy losses and turbulence in sharp open-channel bends. Laboratory experiments, analysis and modelling. *Journal of Geophysical Research – Earth Surface* **114**: F03015. doi:10.1029/2008 JF001137.

Blanckaert, K. 2010. Topographic steering, flow recirculation, velocity redistribution and bed topography in sharp meander bends. *Water Resources Research* **46**: W09506. doi:10.1029/2009WR008303.

Blanckaert, K. and deVriend, H. J. 2004. Secondary flow in sharp open-channel bends. *Journal of Fluid Mechanics* **498**: 353–380.

Blanckaert, K. and deVriend, H. J. 2005a. Turbulence characteristics in sharp open-channel bends. *Physics of Fluids* **17**: 055102–055117.

Blanckaert, K. and de Vriend, H. J. 2005b. Turbulence structure in sharp open-channel bends. *Journal of Fluid Mechanics* **536**: 27–48.

Blanckaert, K., Duarte, A., and Schleiss, A.J. 2010. Influence of shallowness, bank inclination and bank roughness on the variability of flow patterns and boundary shear stress due to secondary currents in straight open channels. *Advances in Water Resources* **33**: 1062–1074. doi:10.1016/j. advwatres. 2010.06.012.

Boyer, C., Roy, A.G., and Best J.L. 2006. Dynamics of a river channel confluence with discordant beds: flow turbulence, bedload sediment transport and bed morphology. *Journal of Geophysical Research – Earth Surface* **111**: F04007. doi:10.1029/2005JF000458.

Boxall, J.B., Guymer, I., and Marion, A. 2003. Transverse mixing in sinuous natural open channel flows. *Journal of Hydraulic Research* **41**: 153–165.

Bradbrook, K.F., Lane, S.N., and Richards, K.S. 2000. Numerical simulation of time-averaged flow structure at river channel confluences. *Water Resources Research* **36**: 2731–2746.

Bradbrook, K. F., Lane, S.N., Richards, K.S., Biron, P.M., and Roy A.G. 2001. Flow structures and mixing at an asymmetrical open-channel confluence: a numerical study, *Journal of Hydraulic Engineering* **127**: 351–368.

Bradshaw, P. 1987. Turbulent secondary flows. *Annual Review of Fluid Mechanics* **19**: 53–74.

Broglia, R., Pascarelli, A., and Piomelli, U. 2003. Large-eddy simulations of ducts with a free surface. *Journal of Fluid Mechanics* **484**: 223–253.

Buffin-Belanger, T.K. Demers, S., and Roy, A. G. 2009. Macroturbulent coherent structures and helical cell motions in an ice-covered meander bend. American Geophysical Union, Fall Meeting 2009, San Francisco, CA. Abstract # EP23B-0629.

Camporeale, C., Perona, P., Porporato, A., and Ridolfi L. 2007. Hierarchy of models for meandering rivers and related morphodynamic processes. *Reviews of Geophysics* **45**: RG1001. doi:10.1029/2005RG000185.

Colombini, M. 1993. Turbulence-driven secondary flows and formation of sand ridges. *Journal of Fluid Mechanics* **254**: 701–719.

Colombini, M. and Parker, G. 1995. Longitudinal streaks. *Journal of Fluid Mechanics* **304**: 161–183.

Constantinescu, S.G., Sukhodolov, A., and McCoy, A. 2009. Mass exchange in a shallow channel flow with a series of groynes: LES study and comparison with laboratory and field experiments. *Environmental Fluid Mechanics* **9**: 587–615. doi: 10.1007/s10652-009-9155-2.

Cooper, J.R. and Tait, S.J. 2008. The spatial organisation of time-averaged velocity and its relationship with the bed surface topography of water-worked gravel beds. *Acta Geophysica*, **56**: 614-642. doi: 10.2478/s11600-008-0023-0.

Cunningham, A. 1883. Recent hydraulic experiments. *Institution of Civil Engineers, Minutes of Proceedings* **71**(Paper No. 1786): 1–36.

Czernuszenko, W. and Rylov, A. 2002. Modeling of three-dimensional velocity field in open channel flows. *Journal of Hydraulic Research* **40**: 135–143.

De Serres, B., Roy, A.G., Biron, P.M., and Best, J.L. 1999. Three-dimensional structure of flow at a confluence of river channels with discordant beds. *Geomorphology* **26**: 313–335.

Demers S., Buffin-Bélanger T., and Roy A.G. 2011. Helical cell motions in a small ice-covered meander river reach. *River Research and Applications* **27**. doi: 10.1002/rra. 1451.

Demuren, A.O. and Rodi, W. 1984. Calculation of turbulence-driven secondary motion in non-circular ducts. *Journal of Fluid Mechanics* **140**: 189–222.

Einstein, H.A. and Li, H. 1958. Secondary currents in straight channels. *American Geophysical Union Transactions* **39**: 1085–1088.

Ettema, R. 2002. Review of River-channel Responses to River Ice. *Journal of Cold Regions Engineering* **16**: 191–217.

Ettema, R. 2008. Ice effects on sediment transport in rivers. In Garcia, M., editor. *Sedimentation Engineering: Processes, Measurements, Modeling, and Practice*. American Society of Civil Engineers, Manuals and Reports on Engineering Practice 110, pp. 613–648.

Ettema, R. and Zabilansky, L. 2004. Ice influences on channel stability: Insights from Missouri's Fort Peck reach. *Journal of Hydraulic Engineering* **130**: 279–292.

Fong, D.A., Monismith, S.G., Stacey, M.T., and Burau, J.R. 2009. Turbulent stresses and secondary currents in a tidal-forced channel with significant curvature and asymmetric bed forms. *Journal of Hydraulic Engineering* **135**: 198–209.

Francis, J.B. 1878. On the cause of the maximum velocity of water flowing in open channels being below the surface. *Transactions of the American Society of Civil Engineers* **7**: 109–113.

Garcia, G. 2008. Sediment transport and morphodynamics. In Garcia, M., editor. *Sedimentation Engineering: Processes, Measurements, Modeling, and Practice*. American Society of Civil Engineers, Manuals and Reports on Engineering Practice 110, pp. 21–164.

Gessner, F.B. 1973. The origin of secondary flow in turbulent flow along a corner. *Journal of Fluid Mechanics* **58**: 1–25.

Gibson, A.H. 1909. On the depression of the filament of maximum velocity in a stream flowing through an open channel. *Proceedings of the Royal Society A. Mathematical and Physical Sciences* **82**: 149–159.

Grega, L.M., Hsu, T.Y., and Wei, T. 2002. Vorticity transport in a corner formed by a solid wall and a free surface. *Journal of Fluid Mechanics* **465**: 331–352.

Gulliver, M. and Halverson, M.J. 1987. Measurements of large streamwise vortices in an open channel-flow. *Water Resources Research* **23**: 115–123.

Gyr, A. 2010. The meander paradox – a topological view. *Applied Mechanics Reviews* **63**: 020801-1.

Hallez, Y. and Magnaudet, J. 2009. Turbulence-induced secondary motion in a buoyancy-driven flow in a circular pipe. *Physics of Fluids* **21**: 081704.

Hinze, J.O., 1967. Secondary currents in wall turbulence. *Physics of Fluids* **10**: S122–S125, doi:10.1063/1.1762429.

Hinze, J.O., 1973. Experimental investigation of secondary currents in the turbulent flow through a straight conduit. *Applied Science Research* **28**: 453–465.

Hurther, D., Lemmin, U., and Terray, E.A. 2007. Turbulent transport in the outer region of rough wall open-channel flows: the contribution of large coherent shear stress structures (LC3S). *Journal of Fluid Mechanics* **574**: 465–493.

Ikeda, S. and Parker, G.editors. 1989. *River Meandering*. American Geophysical Union, Washington, DC.

Ikeda, S. and McEwan, I.K.editors. 2009. *Flow and Sediment Transport in Compound Channels: The Experience of Japanese and UK Research*. International Association for Hydro-environment Engineering and Research (IAHR) Monograph Series. Rotterdam, Balkema.

Jamieson, E.C., Post, G., and Rennie, C.D. 2010. Spatial variability of three-dimensional Reynolds stresses in a developing channel bend. *Earth Surface Processes and Landforms* **35**: 1029–1043.

Joukowski, N.E. 1915. On the water flow at the river bend. *Mathematical Proceedings* **29**. Re-published in Joukowski, N. E. 1937. *Full Collection of Papers*, vol. 4. Moscow-Leningrad, ONTI: 193–233 (in Russian).

Kang, H. and Choi, S.-U. 2009. Scalar flux modeling of solute transport in open channel flows: Numerical tests and effects of secondary currents. *Journal of Hydraulic Research* **47**: 643–655.

Kean, J.W., Kuhnle, R.A., Smith, J.D., Alonso, C.V., and Langendoen, E.J. 2009. Test of a method to calculate near-bank velocity and boundary shear stress. *Journal of Hydraulic Engineering* **135**: 591–601.

Keylock, C.J., Hardy, R.J., Parsons, D.R. *et al.* 2005. The theoretical foundations and potential for large-eddy simulation (LES) in fluvial geomorphic and sedimentological research. *Earth-Science Reviews* **71**: 271–304.

Khosronejad, A., Rennie, C.D., Salehi Neyshabouri, S.A.A., and Townsend, R.D. 2007. 3-D Numerical modeling of flow and sediment transport in laboratory channel bends. *Journal of Hydraulic Engineering* **133**: 1123–1134.

Knight, D.W., Aya, S., Ikeda, S., Nezu, I., and Shiono, K. 2009a. Flow structure. In Ikeda, S. and McEwan, I.K., editors. *Flow and Sediment Transport in Compound Channels: The Experience of Japanese and UK Research*. International Association for Hydro-environmenal Engineering and Research (IAHR) Monograph Series. Rotterdam, A.A.Balkema, pp. 5–113.

Knight, D.W., Ganey, C.M.C., Lamb, R., and Samuels, P.G. 2009b. *Practical Channel Hydraulics*. Amsterdam, Taylor and Francis.

3-DLane, S.N., Bradbrook, K.F., Richards, K.S., Biron, P.M., and Roy, A.G. 1999. Time-averaged flow structure in the central region of a stream confluence: a discussion. *Earth Surface Processes and Landforms* **24**: 361–367.

Lane, S.N., Bradbrook, K.F., Richards, K.S., Biron, P.M., and Roy, A.G. 2000. Secondary circulation in river channel confluences: Measurement myth or coherent flow structure? *Hydrological Processes* **14**: 2047–2471.

Leliavski, N.S. 1894. Currents in streams and the formation of stream beds. *6th International Congress on Navigation Proceedings*. The Hague, The Netherlands.

Levi, E. 1995. *The Science of Water. The Foundation of Modern Hydraulics*. New York, American Society of Civil Engineers Press.

Lyn, D.A. 2008. Turbulence models for sediment transport engineering. In Garcia, M., editor. *Sedimentation Engineering: Processes, Measurements, Modeling, and Practice*. American Society of Civil Engineers, Manuals and Reports on Engineering Practice 110, pp.763–826.

MacVicar, B.J. and Roy, A.G. 2007a. Hydrodynamics of a forced riffle pool in a gravel bed river: 1. Mean velocity and turbulence intensity. *Water Resources Research* **43**: W12401. doi: 10.1029/2006WR05272.

MacVicar, B.J. and Roy, A.G. 2007b. Hydrodynamics of a forced riffle pool in a gravel bed river: 2. Scale and structure of coherent turbulent events. *Water Resources Research* **43**: W12402. doi: 10.1029/2006WR005274.

Marion, A. and Zaramella, M. 2006. Effects of velocity gradients and secondary flow on the dispersion of solutes in curved channels. *Journal of Environmental Engineering* **132**, 1295–1302.

McLean, S.R. 1981. The role of non-uniform roughness in the formation of sand ribbons. *Marine Geology* **42**: 49–74.

McLelland, S.J., Ashworth, P., Best, J.L., and Livesey, J.R. 1999. Turbulence and secondary flow over sediment stripes in weakly bimodal bed material, *Journal of Hydraulic Engineering* **125**: 463–473.

Miyawaki, S., Constantinescu, G., Kirkil, G., Rhoads. B., and Sukhodolov, A. 2009. Numerical investigation of three-dimensional flow structure at a river confluence. *Proceedings of the 33rd IAHR Congress, 9–14 August, Vancouver, Canada (CD ROM)*. International Association for Hydro-environmenal Engineering and Research (IAHR).

Nakagawa, H. and Nezu, I. 1981. Structure of space-time correlations of bursting phenomena in an open-channel flow. *Journal of Fluid Mechanics* **104**: 1–43.

Nezu, I. 2005. Open-channel flow turbulence and its research prospect in the 21st century. *Journal of Hydraulic Engineering* **131**: 229–246.

Nezu, I. and Nakagawa, H. 1993. *Turbulence in Open-Channel Flows*. International Association for Hydraulic Research Monograph Series. Rotterdam, A.A.Balkema.

Nikora, V. 2008. Hydrodynamics of gravel-bed rivers: scale issues. In Habersack, H., Piégay, H. and Rinaldi, M. editors *Gravel-Bed Rivers, Vol. VI*, Amsterdam, Elsevier, Developments in Earth Surface Processes **11**: 61–81.

Nikora, V. 2009. Friction factor for rough-bed flows: interplay of fluid stresses, secondary currents, non-uniformity, and unsteadiness. *Proceedings of the 33rd IAHR Congress, 9–14 August, Vancouver, Canada (CD ROM)*. International Association for Hydro-environmenal Engineering and Research (IAHR).

Nikora V.I., Goring D.G., and Biggs B. *J. F.* 1998. Silverstream eco-hydraulics flume: hydraulic design and tests. *New Zealand Journal of Marine and Freshwater Research* **32**: 607–620.

Odgaard, A.J. and Abad, J.D. 2008. River meandering and channel stability. In Garcia, M., editor. *Sedimentation Engineering: Processes, Measurements, Modeling, and Practice*. American Society of Civil Engineers, Manuals and Reports on Engineering Practice **110**, pp. 439–460.

Papanicolaou, A.N., Elhakeem, M., and Hilldale, R. 2007. Secondary current effects on cohesive river bank erosion. *Water Resources Research* **43**: W12418, doi:10.1029/2006 WR005763.

Parker, G. 2008. Transport of gravel and sediment mixtures. In Garcia, M., editor. *Sedimentation Engineering: Processes, Measurements, Modeling, and Practice*. American Society of Civil Engineers, Manuals and Reports on Engineering Practice **110**, pp. 165–252.

Parsons, D.R., Best, J.L., Lane, S.N. *et al.* 2007. Form roughness and the absence of secondary flow in a large confluence-diffluence, Rio Parana, Argentina, *Earth Surface Processes and Landforms* **32**: 155–162. doi:10.1002/esp.1457.

Pinelli, A., Uhlmann, M., Sekimoto, A., and Kawahara, G. 2010. Reynolds number dependence of mean flow structure in square duct turbulence. *Journal of Fluid Mechanics* **644**: 107–122.

Pizzuto, J.E. 2008. Streambank erosion and river width adjustments. In Garcia, M., editor. *Sedimentation Engineering: Processes, Measurements, Modeling, and Practice*. American Society of Civil Engineers, Manuals and Reports on Engineering Practice **110**, 387–438.

Prandtl, L. 1926. Über die Ausgebildete Turbulenz. In Meissner, E., editor, *2e Internationaler Kongress der Technischen Mechanik*, *Verhandlung*. Füessli, Zürich, 62–75.

Prandtl, L. 1952. *Essentials of Fluid Mechanics*. London and Glasgow, Blackie & Son Ltd.

Rhoads, B. L. and Kenworthy, S.T. 1998. Time-averaged flow structure in the central region of a stream confluence. *Earth Surface Processes and Landforms* **23**: 171–191.

Rhoads, B. L. and Kenworthy, S.T. 1999. On secondary circulation, helical motion, and Rozovskii-based analysis of time-averaged 2-D velocity fields at confluences. *Earth Surface Processes and Landforms* **24**: 369–375.

Rhoads B.L. and Sukhodolov A. 2001. Field investigation of three-dimensional flow structure at stream confluences: Part I. Thermal mixing and time-averaged velocities. *Water Resources Research* **37**: 2393–2410.

Rhoads, B.L. and Welford, M.R. 1991. Initiation of river meandering. *Progress in Physical Geography* **15**: 127–156.

Rice, S.P., Roy, A.G., and Rhoads, B.L., editors. 2008. *River Confluences, Tributaries and the Fluvial Network*. Chichester, John Wiley & Sons, Ltd.

Richardson, W.R. and Thorne, C.R. 2001. Multiple thread flow and channel bifurcation in a braided river: Brahmaputra–Jamuna River, *Bangladesh. Geomorphology* **38**: 185–196.

Rinaldi, M. and Darby, S.E. 2008. Modelling river-bank erosion processes and mass failure mechanisms: progress towards fully coupled simulations. In Habersack, H., Piégay, H., and Rinaldi, M. editors. *Gravel-Bed Rivers VI*. Amsterdam, Elsevier, Developments in Earth Surface Processes **11**: 213–239.

Robinson S.K. 1991. Coherent motion in the turbulent boundary layer. *Annual Review of Fluid Mechanics* **23**: 601–639.

Rodi, W. 1993. *Turbulence Models and their Application in Hydraulics*. International Association for Hydro-environment Engineering and Research (IAHR) Monograph Series. Rotterdam, Balkema.

Rodriguez, J.F. and Garcia, M.H. 2008. Laboratory measurements of 3-D flow patterns and turbulence in straight open channel with rough bed. *Journal of Hydraulic Research* **46**: 454–465.

Rouse, H. and Ince, S. 1963. *History of Hydraulics*. New York, Dover Publications.

Rowiński P.M., Guymer I., and Kwiatkowski K. 2008. Response to the slug injection of a tracer – large scale experiment in a natural river. *Hydrological Sciences Journal* **53**: 1300–1309.

Roy, A.G., Buffin-Belanger, T., Lamarre, H., and Kirkbride, A. D. 2004. Size, shape, and dynamics of large-scale turbulent flow structures in a gravel-bed river. *Journal of Fluid Mechanics* **500**: 1–27.

Rutherford, J.C. 1994. *River Mixing*. Chichester, John Wiley & Sons, Ltd.

Sambrook Smith, G.H., Best, J., Bristow, C.S., and Petts, G.E. 2006. *Braided Rivers: Process, Deposits, Ecology and Management*. International Association of Sedimentologists, Special Publication 36. Chichester, John Wiley & Sons, Ltd.

Sanjou, M. and Nezu, I. 2009. Turbulence structure and coherent motion in meandering compound open-channel flows. *Journal of Hydraulic Research* **47**: 598–610.

Seminara, G. 2006. Meanders. *Journal of Fluid Mechanics* **554**: 271–297.

Seminara, G. 2010. Fluvial sedimentary patterns. *Annual Review of Fluid Mechanics* **42**: 43–66.

Stearns, F.P. 1883. On the current meter, together with a reason why the maximum velocity of water flowing in open channels is below the surface. *Transactions of the American Society of Civil Engineers* **12**: 331–338.

Sterling, M., Beaman, F., Morvan, H., and Wright, N. 2008. Bed shear stress characteristics of a simple, prismatic, rectangular channel. *Journal of Hydraulic Engineering* **134**: 1085–1094.

Stoesser, T., Ruether, N., and Olsen, N.R.B. 2010. Calculation of primary and secondary flow and boundary shear stresses in a meandering channel. *Advances in Water Resources* **33**: 158–170.

Sukhodolov, A. and Kaschtschejewa, E. 2010. Turbulent flow in a meander bend of a lowland river: Field measurements and preliminary results. In Dittrich, A., Koll, Ka., Aberle, J.,and Geisenhainer, P., editors. *River Flow 2010*. Bundesanstalt für Wasserbau, pp. 309–316.

Sukhodolov A. and Rhoads B. 2001. Field investigation of three-dimensional flow structure at stream confluences: Part II. *Turbulence. Water Resources Research* **37**: 2411–2424.
Szupiany, R.N., Amsler, M.L., Parsons, D.R., and Best, J.L. 2009. Morphology, flow structure, and suspended bed sediment transport at two large braid-bar confluences. *Water Resources Research* **45**: W05415. doi:10.1029/2008WR007428.
Tennekes, H. and Lumley, J.L. 1972. *A First Course in Turbulence*. Cambridge, MA, MIT Press.
Termini, D. 2009. Experimental observations of flow and bed processes in large-amplitude meandering flume. *Journal of Hydraulic Engineering* **135**: 575–587.
Thomson, J.J. 1876. On the origin of windings of rivers in alluvial plains, with remarks on the flow of water round bends in pipes. *Proceedings of the Royal Society of London* **25**: 5–8. Re-published in *Nature* **122**: 14 (1976).
Townsend, A.A. 1976. *The Structure of Turbulent Shear Flow*. Cambridge, Cambridge University Press.
Tsai, W.-F. and Ettema, R. 1994. Ice cover influence on transverse bed slopes in a curved alluvial channel. *Journal of Hydraulic Research* **32**: 561–582.
Tsinober, A. 2009. *An Informal Conceptual Introduction to Turbulence*. Dordrecht, Springer.
Van Balen, W., Uijttewaal, W.S.J., and Blanckaert, K. 2009. Large-eddy simulation of a mildly curved open-channel flow. *Journal of Fluid Mechanics* **630**: 413–442.
Van Balen, W., Blanckaert, K., and Uijttewaal, W.S.J. 2010. Analysis of the role of turbulence in curved open-channel flow at different water depths by means of experiments, LES and RANS. *Journal of Turbulence* **11**: Article no. 12. doi: 10.1080/14685241003789404.
Vanoni, V.A. 1946. Transportation of suspended sediment by water. *Transactions of the American Society of Civil Engineers* **111**: 67–133.
Wang, Z-Q. and Cheng, N.-S. 2006. Time-mean structure of secondary flows in open channel with longitudinal bedforms. *Advances in Water Resources* **2**: 1634–1649.
Wood, D.V. 1879. On the flow of water in rivers. *Transactions of the American Society of Civil Engineers* **8**: 173–178.
Yang S.-Q., 2005. Interactions of boundary shear stress, secondary currents and velocity. *Fluid Dynamics Research* **36**: 121–136.
Yang, S.-Q. and Lim, S.-Y. 1997. Mechanism of energy transportation in a 3-D channel. *Journal of Hydraulic Engineering* **123**: 684–692.
Yen, B.C. 2002. Open channel flow resistance. *Journal of Hydraulic Engineering* **128**: 20–39.
Zeng, J., Constantinescu, G., Blanckaert, K., and Weber, L. 2008. Flow and bathymetry in sharp open-channel bends: Experiments and predictions. *Water Resources Research* **44**: W09401. doi:10.1029/2007 WR006303.
Zeng, J., Constantinescu, G., and Weber, L. 2010. 3-D calculations of equilibrium conditions in loose-bed open channels with significant suspended sediment load. *Journal of Hydraulic Engineering* **136**: 557–571.

1.10 DISCUSSION

1.10.1 Discussion by Tim Randle

Would the authors please comment on the potential for secondary currents of the second kind in straight channels (e.g. canals, straightened channels, perhaps meander cutoffs) to eventually evolve the channel platform to increased sinuosity and the development of secondary currents of the first kind?

1.10.2 Discussion by Gordon E. Grant

Is it possible to use our current understanding and ability to model secondary flows to establish a set of criteria (or even a set of hypotheses) about where such flows should and should not have morphodynamic significance? In other words, it's one thing to be able to identify that secondary flows, perhaps as stimulated by grain roughness or similar, should exist; it's another to argue that such flows should leave a discernible and measureable imprint on the channel morphology. For example, in very rough channels, any tendency for coherent secondary flow structures is likely to be suppressed by the turbulence set up by the form and large-scale grain roughness. It would help us better understand secondary flows and their role in channel morphology if we could identify, at least to first order, where we should expect to see coherent flow structures that could potentially modify channel form.

1.10.3 Reply by Vladimir Nikora and André G. Roy

T. Randle's question and G. Grant's comment highlight a potentially important role of secondary currents in generating instabilities in channels with erodible boundaries. For example, a time-averaged secondary cell in a straight channel can be viewed as a manifestation of the frequently occurring instantaneous helical motions, wandering, to a certain degree, across the channel and serving as large-scale perturbations leading to development of plane deformations of the channel. A similar situation may also occur in channels with more realistic and complex channel geometries, with different types of secondary currents. Recent achievements in this field suggest that soon we should have much better capabilities for predicting locations and strength of time-averaged secondary currents. However, it seems that the role of the mean secondary currents in channel morphodynamics is essentially defined by their instantaneous components (e.g., helical motions), regularly or intermittently occurring in the flow. We believe that the topology, intensity, and statistics of these instantaneous components of the time-averaged secondary currents, still practically unknown, will provide important knowledge to better understand many aspects of channel morphodynamics.